Paleoceanography and Paleoclimatology

RESEARCH ARTICLE
10.1029/2019PA003661

Early Interglacial Legacy of Deglacial Climate Instability

Stephen Barker[1], Gregor Knorr[1,2], Stephen Conn[1], Sian Lordsmith[1], Dhobasheni Newman[1], and David Thornalley[3]

[1]School of Earth and Ocean Sciences, Cardiff University, Cardiff, UK, [2]Alfred Wegener Institute, Bremerhaven, Germany, [3]Department of Geography, University College London, London, UK

Key Points:
- The relationship between changes in atmospheric CO_2 and surface conditions across the NE Atlantic has been consistent over the past 800 kyr
- The ocean/atmosphere system may take thousands of years to reequilibrate following abrupt deglacial oscillations in ocean circulation
- Inclusion of nonequilibrium intervals within interglacial comparisons may lead to artifacts in calculated trends in, for example, atmospheric CO_2

Supporting Information:
- Supporting Information S1
- Data Set S1

Correspondence to:
S. Barker,
barkers3@cf.ac.uk

Citation:
Barker, S., Knorr, G., Conn, S., Lordsmith, S., Newman, D., & Thornalley, D. (2019). Early interglacial legacy of deglacial climate instability. *Paleoceanography and Paleoclimatology*, *34*, 1455–1475. https://doi.org/10.1029/2019PA003661

Received 17 MAY 2019
Accepted 2 AUG 2019
Accepted article online 9 AUG 2019
Published online 24 AUG 2019

Abstract Throughout the last glacial cycle millennial timescale variations in atmospheric CO_2 occurred in parallel with perturbations in deep ocean circulation, which were themselves reflected by observable changes in surface conditions across the North Atlantic region. Here we use continuous proxy records to argue that an equivalent relationship has held throughout the last 800 kyr, that is, since before the first occurrence of Heinrich events (strictly defined). Our results highlight the importance of internal climate dynamics in amplifying external (insolation) forcing on the climate system to produce the large amplitude of glacial terminations (deglaciations) during the middle to late Pleistocene. We show that terminations are characterized by an interval of intense ice rafting followed by a subsequent and abrupt shift to anomalously warm surface conditions (with respect to the more gradually evolving background state), which we interpret to reflect an abrupt recovery of deep ocean circulation in the Atlantic. According to our synthesis, this is followed by a period of enhanced (or at least anomalous) overturning lasting thousands of years until equilibrium interglacial conditions are attained and during which atmospheric CO_2 is likely to decrease. Our results therefore suggest that deglacial oscillations in ocean circulation can have a lasting influence on early interglacial climate and highlight the transient nature of atmospheric CO_2 overshoots associated with the onset of some previous interglacials. Accordingly, we suggest that these intervals should be considered as a part of the deglacial process. This has implications for studies concerned with the evolution of atmospheric CO_2 during interglacial periods including the Holocene.

1. Introduction

This work is dedicated to the memory of Wallace S. Broecker, a friend and mentor, whose impact on paleoceanography and the study of paleoclimate was profound. It is humbling to consider how often we seem to repaint the wheels invented by past leaders in our respective fields. Wally's tracks appear most often within texts on glacial-interglacial CO_2 variability, abrupt climate change, and ocean circulation, and it seems appropriate then that his 1989 study with George Denton provided such clear foresight to the conclusions of this study.

Reconstructions of ocean circulation and the record of atmospheric CO_2 across Marine Isotope Stage (MIS) 3 and the last deglaciation (Termination, T1) reveal a close coupling between ocean state and CO_2 (Figures 1–3) with CO_2 rising (on a millennial timescale), while Atlantic Ocean circulation (specifically the Atlantic Meridional Overturning Circulation, AMOC) is in a pronounced weak or shallow mode (particularly those intervals associated with so-called Heinrich events-massive North Atlantic ice rafting events sourced from Hudson Strait (Hemming, 2004)) and decreasing again after recovery to a strong mode, at least during MIS 3 (Ahn & Brook, 2008; Henry et al., 2016; Marcott et al., 2014; Roberts et al., 2010). An additional century scale rise in CO_2 may also occur as the AMOC recovers (Chen et al., 2015; Deaney et al., 2017; Marcott et al., 2014). Modeling studies suggest that such changes in CO_2 could be driven by biophysicochemical changes directly associated with variations in deep ocean circulation (Ganopolski & Brovkin, 2017; Kohler et al., 2005; Marchal et al., 1998; Menviel et al., 2014; Schmittner & Galbraith, 2008; Sigman et al., 2010) or indirectly through affiliated changes in atmospheric circulation (Menviel et al., 2008). For the purposes of this study, however, it is the temporal association between changes in ocean circulation and atmospheric CO_2 (implying a mechanistic link) that is of critical interest; we wish to determine whether or not this association has been consistent over the last 800 kyr, during which we have continuous records of atmospheric composition and encompassing a period before the appearance

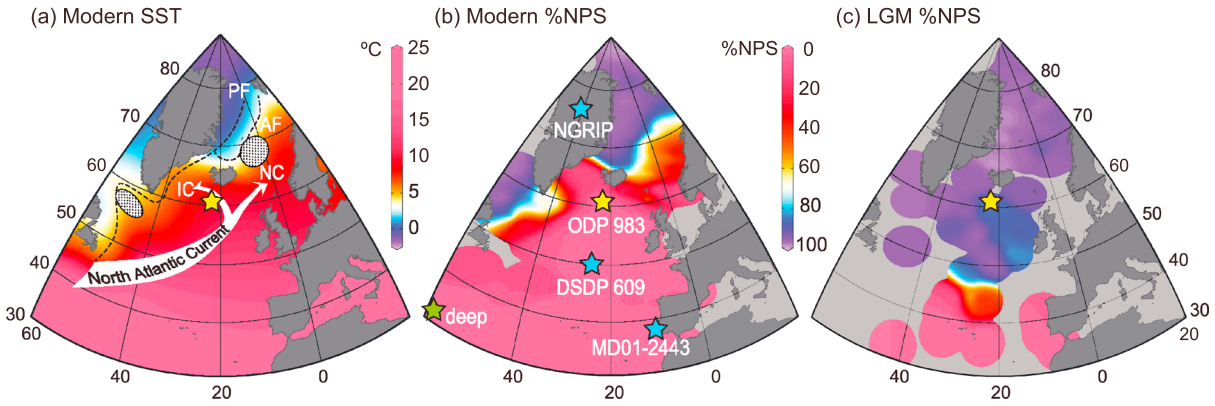

Figure 1. Location Map. (a) Modern annual sea surface temperatures (SSTs; Locarnini et al., 2010) reflect the transport of heat into the Nordic Seas via the North Atlantic Current (i.e., the Nordic heat pump; see section 3.3), which splits into the Irminger Current (IC) and Norwegian Current (NC). Hatched areas are approximate regions of modern deep water formation. Sites mentioned in the study (ODP 983, DSDP 609, MD01-2443, and NGRIP) are highlighted, as is the location of several deep ocean circulation reconstructions (green star; McManus et al., 2004; Roberts et al., 2010; Henry et al., 2016; Deaney et al., 2017). PF and AF are Polar and Arctic Fronts. (b) Modern (cope-top) distribution of *Neogloboquadrina pachyderma* (%NPS; Margo_Project_Members, 2009) reflects the SW-NE orientation of Polar and Arctic Fronts. (c) LGM distribution of %NPS (Margo_Project_Members, 2009) suggests southward shift of fronts and by implication a weakened Nordic heat pump. Maps were created with the ODV application (Schlitzer, 2014).

of Heinrich events in a strict sense (i.e., derived from Hudson Strait) around 640 ka (Hodell et al., 2008; Naafs et al., 2011).

An initial test of this proposition is given by a comparison between changing atmospheric CO_2 and a reconstruction of northern abrupt climate variability, GL_T_syn_hi (Barker et al., 2011), which we argue provides a zeroth-order approximation for AMOC strength (see section 2.3 and Figure 4). The comparison suggests that a major proportion of CO_2 change (in either direction) occurs when the AMOC is furthest from equilibrium. In particular, CO_2 tends to increase while the AMOC is (inferred to be) anomalously weak and decrease when the AMOC is (inferred to be) anomalously strong. Ahn and Brook (2014) demonstrated that atmospheric CO_2 does not necessarily change during shorter stadial events, and our analysis does not contradict this. Figure 4 suggests that >50% of the cumulative rise in CO_2 over the last 800 kyr coincided with strongly negative values of GL_T_syn_hi (which should coincide with stadial conditions across the North Atlantic), but we also note that many instances of negative GL_T_syn_hi coincide with unchanging or even decreasing CO_2.

Within this study we use the term “equilibrium” (and “quasi-equilibrium”) to reflect a (hypothetical) situation where the climate system (including all its components e.g., mean temperature, ocean circulation, atmospheric CO_2 concentration) is equilibrated (or close to being equilibrated) with respect to Earth's orbital configuration. Since Earth's orbit varies continuously, we would not expect equilibrium conditions to remain constant but instead to vary on timescales $>10^3$ years. Furthermore, thanks to the inherent nonlinearity of Earth's climatic response to changes in insolation (see below), it is difficult to assess whether any observed climate “state” (e.g., glacial or interglacial) represents anything like a truly equilibrated state. We therefore use the term with caution, but nevertheless, we think it is useful in the context of millennial-scale variability. We also define “anomaly” as the difference (departure) from more gradually evolving background conditions, in this case a 7 kyr smooth of the record under consideration (see section 2.2.1). In this context, background conditions can be considered as broadly synonymous with equilibrium conditions.

Milankovitch (1941) predicted that changes in the integrated intensity of Northern Hemisphere summer insolation should drive the waxing and waning of continental ice sheets and ultimately the transitions between glacial and interglacial states. However, the forcing due to changing summer insolation alone is not sufficient to explain the large magnitude of deglacial transitions (Imbrie et al., 1993; known as glacial terminations; Broecker & van Donk, 1970) and it has long been appreciated that nonlinearities within the climate system are required in order to explain the magnitude of these major climate shifts. Early work suggested that abrupt changes in ocean circulation and their influence on atmospheric CO_2 could play a central

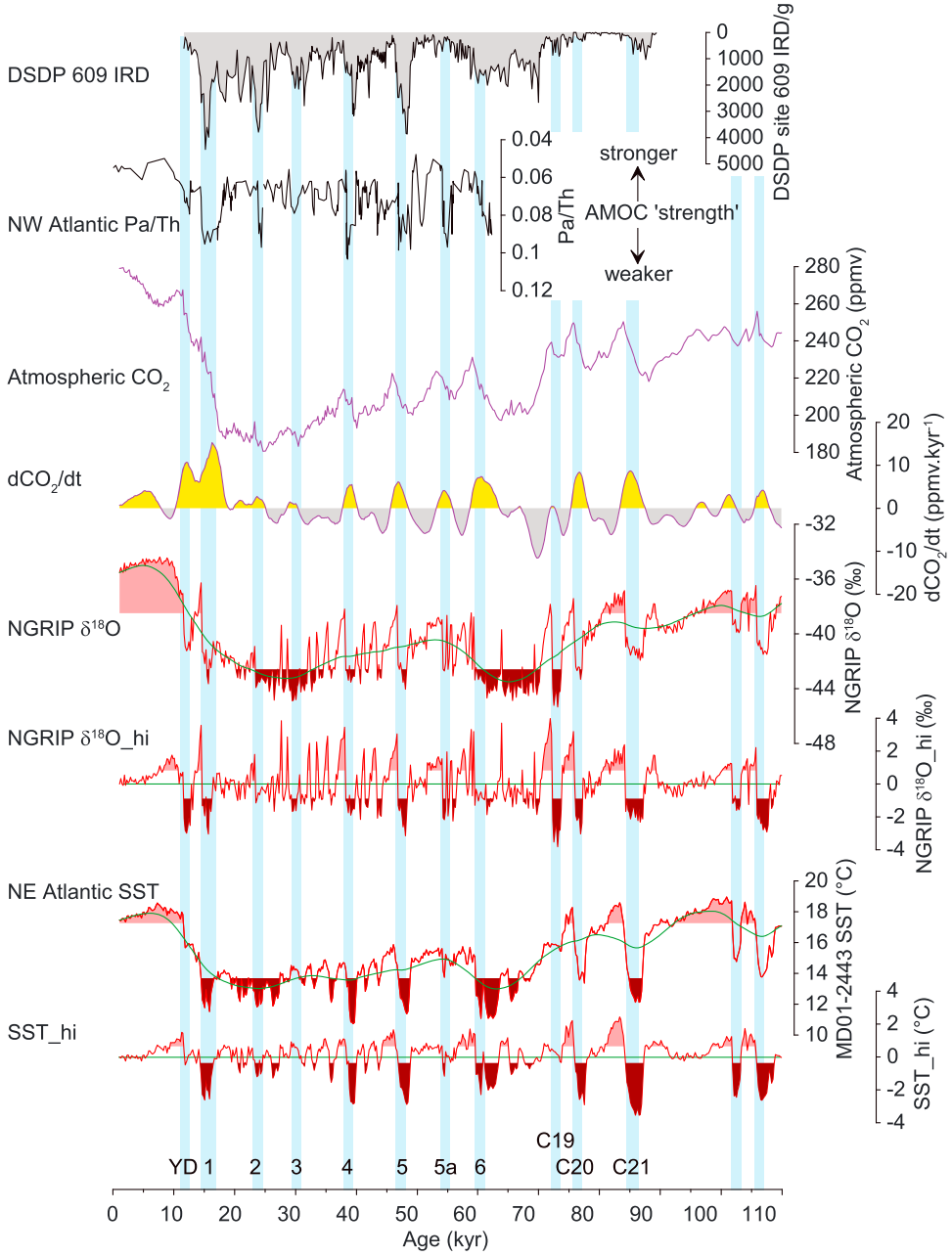

Figure 2. Changing atmospheric CO_2 and ocean conditions over the last 110 kyr (see Figure 1 for locations). From top to bottom: Records of IRD from DSDP site 609 (Bond & Lotti, 1995), sedimentary Pa/Th from the deep NW Atlantic (a proxy for AMOC strength; McManus et al., 2004; Böhm et al., 2015; Henry et al., 2016), atmospheric CO_2 (Bereiter et al., 2015), dCO_2/dt (section 2.2), NGRIP $\delta^{18}O$ (NGRIP_members, 2004), and NGRIP $\delta^{18}O$_hi (section 2.2.1), SST from MD01-2443 (Martrat et al., 2007), SST_hi. Numbered blue boxes represent cold (Heinrich) stadial periods. For lower four curves, dark pink areas represent the coldest quartile (25% of time) and light pink the warmest quartile. These relate to Classes 1 and 4, respectively in Figure 3. IRD = ice rafted debris; AMOC = Atlantic Meridional Overturning Circulation; SST = sea surface temperature.

role in the mechanism of termination (Broecker & Denton, 1989; Imbrie et al., 1993), and several recent studies have reached an equivalent conclusion based on evidence from various paleoclimate archives (Anderson et al., 2009; Barker et al., 2009; Barker et al., 2011; Cheng et al., 2009; Cheng et al., 2016; Denton et al., 2010; Skinner et al., 2010). Specifically, a shift in ocean circulation patterns during

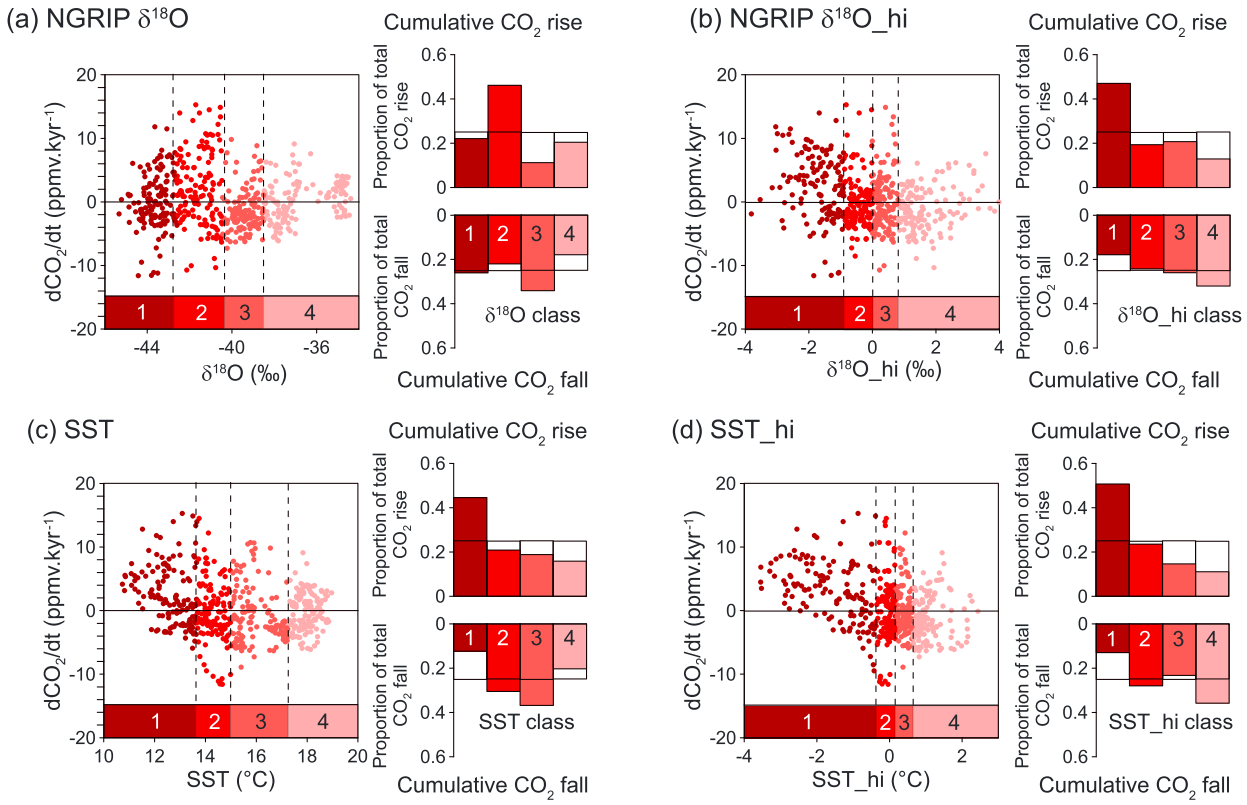

Figure 3. Changing CO_2 versus surface ocean conditions as shown in Figure 2. (a, left) Rate of change of atmospheric CO_2 versus NGRIP $\delta^{18}O$ for discrete 200-year intervals. Colored classes represent 25% of the population (i.e., a quarter of the time). (Right) Distribution of cumulative CO_2 rise (upper) and fall (lower) across NGRIP $\delta^{18}O$ classes as defined in (a, left) over the past 110 kyr (horizontal lines at ±0.25 indicate expected value if there were no systematic relationship). (b) Same as (a) but for NGRIP $\delta^{18}O$_hi. (c, d) Same as (a, b) but for MD01-2443 SST and SST_hi. See section 2.2 for explanation. SST = sea surface temperature.

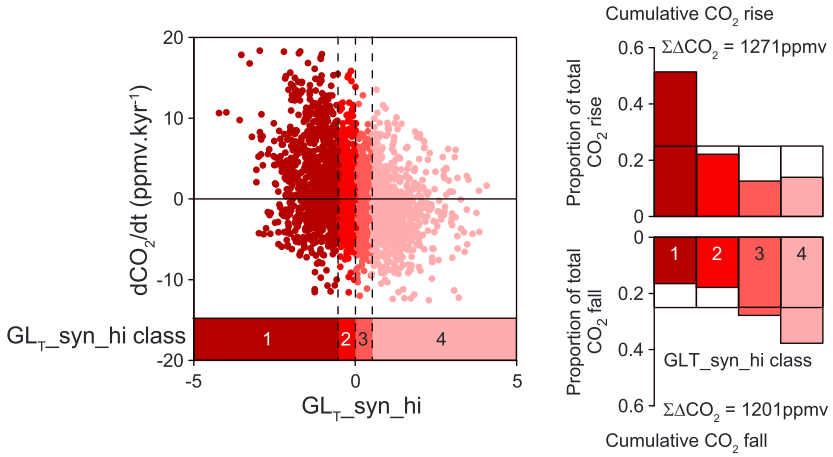

Figure 4. Rate of change of atmospheric CO_2 versus GL_T_syn_hi for discrete 200-year intervals over the past 800 kyr. Colored classes represent 25% of the population (i.e., a quarter of the time). (Right) Distribution of cumulative CO_2 rise (upper) and fall (lower) across GL_T_syn_hi classes over the past 800 kyr. High absolute values of GL_T_syn_hi (e.g., Classes 1 and 4) represent intervals when the AMOC is furthest from equilibrium, that is, anomalously weak (negative GL_T_syn_hi, class 1) or strong (Class 4; see section 2.3). Note similarity with right-hand panels of Figures 3b and 3d, which represent only the last 110 kyr.

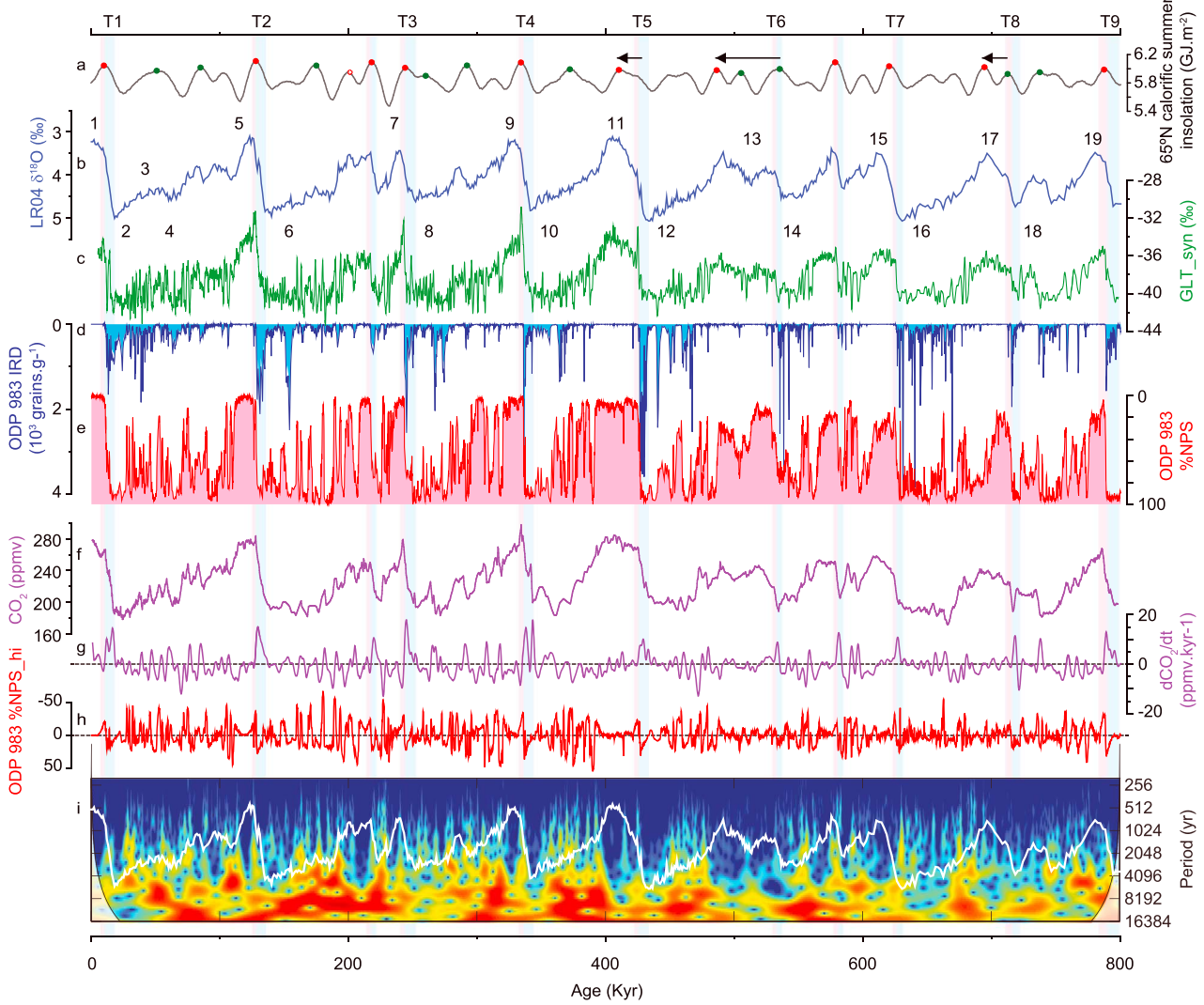

Figure 5. The last 800 kyr of abrupt climate variability. (a) Integrated northern summer insolation (black curve; Tzedakis et al., 2017). (b) Benthic foraminiferal $\delta^{18}O$ stack (blue; Lisiecki & Raymo, 2005). (c) GL_T_syn, a prediction of northern abrupt climate variability (green; Barker et al., 2011). (d, e) IRD/g (blue filled) and %NPS (pink filled) from ODP site 983. (f, g) atmospheric CO_2 and dCO_2/dt (purple). (h) %NPS_hi (red; section 2.2.1). (i) Wavelet transform of %NPS, produced using the Matlab function given by Grinsted et al. (2004) and implemented on the %NPS record after evenly resampling at 100-year intervals (white curve is the LR04 benthic stack). T1-9 are glacial terminations; #1–19 are MIS; colored boxes as in Figure 7 annotation. Red and green circles in (a) are peaks in summer energy that (respectively) do and do not cross the threshold for producing an interglacial state (Tzedakis et al., 2017). T6 and T8 represent protracted terminations (see text).

termination is thought to lead to an increase in CO_2 that can eventually promote the transition to an interglacial state. Here we wish to investigate this link for all of the deglacial transitions of the last 800 kyr. In particular, we are interested in the similarities and differences among individual terminations and whether these impact the climatic evolution of subsequent interglacial periods.

The gradual rise in atmospheric CO_2 throughout the last 8,000 years of the Holocene (prior to industrialisation) has attracted many possible explanations, ranging from natural (e.g., through changes in the terrestrial biosphere or marine inorganic chemistry; Indermühle et al., 1999; Broecker et al., 2001; Ridgwell et al., 2003; Elsig et al., 2009; Kleinen et al., 2010) to anthropogenic influences such as deforestation (Ruddiman, 2003; Ruddiman et al., 2016). Ruddiman et al. (2016) use various comparisons between the Holocene (MIS 1) and earlier interglacials to argue that the Holocene (upward) trend in CO_2 is anomalous and therefore unnatural or anthropogenic. However, according to their analysis, only three interglacials (MIS 7, 9, and 19) consistently reveal a decreasing trend (with the additional possibility of MIS 5). Notably, these interglacials are themselves unusual because they display so-called overshoots in CO_2 at

their onset (Tzedakis et al., 2009; Figure 5). If these overshoots actually reflect the transient effects of abrupt deglacial changes in ocean circulation (rather than quasi-equilibrium interglacial conditions) then it could be argued that they should not be included in the definition (and therefore analysis) of interglacial trends in CO_2 in which case the conclusions of Ruddiman et al. (2016) may have to be moderated. A recent modeling study by Ganopolski and Brovkin (2017) suggests this might be the case. These authors conclude that the timing of AMOC recovery within a termination is critical for determining the early interglacial level of atmospheric CO_2. For example, if recovery occurs only at the end of termination (e.g., when CO_2 has already reached an interglacial level), a pronounced overshoot in CO_2 will occur, followed by a steady or decreasing trend during the subsequent interglacial (e.g., MIS 5). On the other hand an early AMOC recovery will result in a lower initial CO_2 level, followed by a rise during the subsequent interglacial (e.g., MIS 1). A similar conclusion was reached in a proxy study by Deaney et al. (2017), who suggested that the early AMOC recovery associated with the Bølling-Allerød during Termination 1 could explain the smaller apparent magnitude of CO_2 change across T1 as compared with the previous deglaciation (T2) for which AMOC recovery did not occur until the very end of termination, resulting in a transient CO_2 overshoot associated with AMOC recovery during early MIS 5.

To test these ideas more thoroughly requires (ideally) high-resolution reconstructions of ocean circulation across multiple terminations as well as during glacial and interglacial periods to assess the connection between ocean circulation and CO_2 change for a variety of timescales and background states. However, unambiguous reconstructions of deep ocean circulation are difficult to obtain and as a result, direct evidence for a temporal link between changes in ocean circulation and atmospheric CO_2 across deglacial transitions is currently limited to the last two terminations (T1 and T2; Roberts et al., 2010; Deaney et al., 2017). However, the observed correlation between ocean circulation and surface conditions across the North Atlantic region over the last glacial cycle (weakened circulation is associated with ice rafting and anomalously cold conditions and vice versa; Figure 2) allows a first-order approximation of the relationship between the AMOC and atmospheric CO_2 over this interval to be made using surface conditions as a surrogate for the state of ocean circulation (section 2.2 and Figure 3). In general, CO_2 tends to increase while the North Atlantic region is anomalously cold (reflecting periods of weakened AMOC) and decrease when conditions are anomalously warm (when Atlantic circulation is relatively strong). Note again that we are interested in the temporal relationship between CO_2 and AMOC; this discussion does not address the specific mechanism linking ocean circulation to CO_2 (i.e., it does not imply that a weakening of AMOC directly causes an increase in CO_2 or vice versa).

In this study we aim to exploit this observation to investigate the relationship between ocean circulation and changing atmospheric CO_2 over the past 800 kyr, using proxies for NE Atlantic surface conditions from ODP site 983 (Figure 1) as a surrogate for the state of ocean circulation within the Atlantic (i.e., strength of the AMOC). Several statistical and modeling studies have suggested a direct link between temperature variations in the subpolar North Atlantic and the strength of AMOC (Caesar et al., 2018; Dima & Lohmann, 2010; Muir & Fedorov, 2015; Zhang, 2008) with observational support for this relationship deriving from the RAPID-AMOC 26°N array (Smeed et al., 2018). Cooling of the subpolar gyre over the last millennium is thought to be a direct manifestation of weakening AMOC strength (Caesar et al., 2018; Rahmstorf et al., 2015; Thornalley et al., 2018), and this is supported by reconstructions of the Deep Western Boundary Current over the same period (Thornalley et al., 2018). ODP Site 983 is located within the region of subpolar cooling associated with recent AMOC weakening (Caesar et al., 2018; Smeed et al., 2018), and therefore, we suggest that it is in a suitable position for assessing past changes in AMOC strength using this approach. We employ the relative proportion of *Neogloboquadrina pachyderma* (a polar-affiliated species of planktic foraminifera) within the total assemblage (%NPS) to reconstruct fluctuations between polar and subpolar conditions and the millennial-scale component of this (%NPS_hi; section 2.2.1) to identify periods of anomalous cold and warmth. We also use the concentration of lithic grains >150 μm (ice rafted debris, IRD) to reflect the transport of icebergs to the open ocean southwest of Iceland. The limitations of our approach are obvious (we are using a single core site to estimate large scale change in AMOC by means of an indirect approach), but we maintain that at the very least our assessment of the link between surface conditions in the NE Atlantic and changes in atmospheric CO_2 will provide a valuable test for climate models and a testing ground for a range of future proxy studies.

2. Materials and Methods

2.1. Sample Preparation and Age Model for ODP Site 983

For this study we processed 2,272 samples along the splice of ODP 983 (Jansen et al., 1996). Each sample was 2 cm wide (representing ~170 years on average), taken every 2 cm from 0.02 to 1.98 and 51.52 to 94.95 MCD. Previously (Barker et al., 2015), we reported results from the interval 2.0 to 51.5 MCD. Sediment samples were spun overnight and washed with DI water through a 63-μm sieve before being dried at 40 °C. IRD and faunal counts were made on the >150-μm fraction after splitting to yield approximately 300 entities. IRD was considered as the total number of lithogenic/terrigenous grains counted. The majority of grains fall into two categories: quartz and volcanics, with volcanics comprising ~36% of the total IRD on average during the last glacial period (Barker et al., 2015). Only left coiling specimens of *N. pachyderma* were counted, and all five morphotypes of *N. pachyderma* found in recent Arctic sediments (Eynaud, 2011) were counted (Figure S1 in the supporting information). We recounted ~1,000 of the samples previously reported (Barker et al., 2015) covering the depth interval 32.04 to 51.5 MCD because of concerns over nonidentification of lightly encrusted morphotypes of *N. pachyderma* during the warm stages of MIS 11 (Figure S2). Our recounts suggest that we had previously underestimated the proportion of *N. pachyderma* during MIS 11 but were correctly calibrated in later warm intervals. We also checked our taxonomy across MIS 11 by resampling nearby ODP site 980 that was analyzed by Oppo et al. (1998). Our counts are in very good agreement with that study (Figure S2). We stress that our recounts do not affect the conclusions of our previous study (Barker et al., 2015).

The site of ODP site 983 is positioned on the rapidly accumulating Gardar Drift, and sediment accumulation is sensitive to changes in the dense overflows crossing the Iceland-Scotland Ridge (Kleiven et al., 2011; Raymo et al., 2004) which themselves are thought to covary with high-latitude climate (Ezat et al., 2014; Kleiven et al., 2011). At orbital timescales this results in elevated sedimentation rates during interglacials (as implied by the LR04 age model; Lisiecki & Raymo, 2005, and noted previously; Barker et al., 2015) when the overflows are thought to be more vigorous (Kleiven et al., 2011; Raymo et al., 2004). But this also implies that sedimentation rates are elevated during millennial-scale warm events that are not accounted for by the LR04 age model. It is therefore necessary to tune our records to a target with millennial-scale features, and following our previous study (Barker et al., 2015), we use the millennial component of a synthetic reconstruction of northern climate variability (GL_T_syn_hi) (Barker et al., 2011) derived from the Antarctic ice core temperature record (Jouzel et al., 2007) on the AICC2012 age model (Bazin et al., 2013) as a tuning target (Figure S3). Specifically, we align abrupt warming events in our record (which also align with the disappearance of IRD) with warming transitions in GL_T_syn_hi. We also align increases in the coarse fraction (>63 μm) with cooling transitions in GL_T_syn_hi. The coarse fraction of ODP 983 reflects both the delivery of IRD (which increases during stadials) and the input of fine fraction (which decreases during stadials due to reduced advection of fine material to ODP site 983 by slower currents crossing the Iceland-Faeroe ridge; Raymo et al., 2004).

IRD accumulation rates were calculated from IRD/g and dry bulk accumulation rates, obtained by combining linear sedimentation rates with an estimate for dry bulk density, derived from continuous GRAPE (Gamma-Ray Attenuation Porosity Evaluator; Evans, 1965) density (ρ_{GRAPE}) measurements calibrated with discrete (index property) measurements of wet and dry bulk density (Jansen et al., 1996)

$$\text{Dry Bulk Density} = (\rho_{GRAPE} + 0.17)*1.5547-1.5719 \quad (1)$$

2.2. Changing CO_2 Versus Surface Conditions Across the North Atlantic Region

For comparisons among data sets, individual records were resampled onto a common timescale with a 200-year time step. In addition, the record of atmospheric CO_2 (Bereiter et al., 2015) was smoothed using a running mean of 2 kyr prior to differentiation (note that this limits our analysis to millennial-scale changes in CO_2). The age model for the CO_2 record is AICC2012 (Bazin et al., 2013; Veres et al., 2012), slightly modified according to Method 4 of Parrenin et al. (2012) for determination of gas-ice depth differences (Δdepth) along the EDC ice core by alignment of CH_4 with deuterium isotope maxima. This is considered preferable to model-based estimates of Δdepth in the deeper parts of the ice core.

2.2.1. Defining Anomalous Conditions

Proxies for surface temperature (%NPS in ODP 983, sea surface temperature [SST] in MD01-2443; Martrat et al., 2007, and $\delta^{18}O$ in the NGRIP ice core; NGRIP_members, 2004) are expressed as an anomaly with respect to background conditions (by subtraction of a 7-kyr running mean) in order to isolate millennial-scale variability for comparison to the record of dCO_2/dt. The effect of this operation is equivalent to the 7-kyr "orbital filter" applied in previous studies (Alley et al., 2002; Barker et al., 2011; Schmittner et al., 2003) and is particularly important in records where millennial-scale variations may be less pronounced than orbital timescale (G-IG) changes. For example, in the unfiltered record of Greenland $\delta^{18}O$ (Figure 2) the coldest (lowest $\delta^{18}O$) and warmest (highest $\delta^{18}O$) quartiles (25% of the time) approximate to glacial and interglacial conditions, respectively. Thus, even though CO_2 is known to increase during the pronounced (cold) stadials of MIS 3 and the last deglaciation (i.e., H-stadials), this is not reflected by the direct comparison of changing CO_2 with NGRIP $\delta^{18}O$ (Figure 3a). In contrast, for the hi-pass filtered record (NGRIP $\delta^{18}O$_hi) the coldest (lowest $\delta^{18}O$_hi) and warmest (highest $\delta^{18}O$_hi) quartiles more closely reflect stadial and interstadial periods, respectively (Figure 2), which better differentiates between intervals of CO_2 increase and decrease. In this case (Figure 3b), and in agreement with expectations, CO_2 tends to increase during the coldest quartile ($\delta^{18}O$_hi Class 1) and decrease during the warmest quartile ($\delta^{18}O$_hi Class 4).

It has been suggested that subtraction of a running mean as described will produce "artificial" millennial-scale events during transitions between, for example, glacial and interglacial states. For example, if a shift from a long period of low %NPS to a long period of high %NPS (e.g., that associated with a deglacial transition) occurs within a few hundred years, then subtraction of a 7-kyr running mean will produce a millennial-scale oscillation (from anomalously cold to anomalously warm) in the calculated anomaly while the raw data show no such feature (merely a stepwise transition from low to high). But this is exactly the definition of anomaly that we intend; it is the anomaly with respect to background conditions (defined here by a 7-kyr running mean). To give an analogous example, it is commonly thought that the AMOC experienced a weakening associated with Heinrich events during MIS 3 and the last deglaciation (Henry et al., 2016; McManus et al., 2004). It can be said that the AMOC was anomalously weak during those events, and we also observe that atmospheric CO_2 tended to increase during those same events (Ahn & Brook, 2008; Marcott et al., 2014). Now, if a period of weakened AMOC lasted for several thousands of years, then presumably at some point we could no longer consider such conditions as anomalous (since they would represent the "new normal"). Furthermore, we would probably not expect CO_2 to keep increasing for however long the AMOC remained in a weakened state (at some point we would expect the level of atmospheric CO_2 to reach a new equilibrium). But does this mean therefore that we should not consider as anomalous the period directly following the initial weakening? We contend that we should. By analogy, we argue that the millennial-scale events in the record of %NPS_hi are not merely fortuitous artifacts of our numerical procedure but by our definition represent periods of anomalous conditions at the site of ODP 983.

Our specific choice of a 7-kyr running mean to isolate millennial-scale variability is guided by previous studies (Alley et al., 2002; Barker et al., 2011; Schmittner et al., 2003), and we suggest that this choice reasonably represents background climate evolution on G-IG timescales. Use of a shorter timescale could be argued for from a purely oceanic perspective (perhaps 1–2 kyr or more; Yang & Zhu, 2011; Jansen et al., 2018) as could a longer timescale to account for complete equilibration of land-based ice sheets (perhaps 10 kyr). In Figure S4 we demonstrate the effect of different smoothing windows on the derived record of %NPS_hi. Varying the smoothing window from 2 to 10 kyr actually produces quite similar results, with the main effect being shorter and more accentuated (with respect to other millennial events) early interglacial anomalies when using a shorter smoothing window (except when a pronounced millennial-scale event occurs in the unprocessed record as in T2, when all records look practically identical). In any case when defining the duration of anomalous conditions at the onset of interglacial periods, we employ the records of benthic foraminiferal $\delta^{13}C$ (from the same site) and GL_T_syn_hi (derived from the Antarctic ice core record) together with %NPS_hi (Figure S4; sections 4.1 and 4.2).

2.3. GL_T_syn_hi as a Zeroth-Order Approximation for AMOC Strength

The inverse relationship observed between millennial-scale temperature anomalies in the Greenland ice core record (i.e., cold stadials and warm interstadials) and the rate of change of Antarctic temperature has been used to argue for involvement of ocean circulation (specifically the AMOC) in abrupt climate change

(Barker et al., 2011; Schmittner et al., 2003; Stocker & Johnsen, 2003). On the other hand it has also been suggested that the comparatively small contribution of the ocean to the net meridional heat flux makes it unlikely that changes in the AMOC would give rise to major changes in climate and moreover that any reduction in northern oceanic heat transport would be compensated by a corresponding increase in atmospheric transport (Wunsch, 2006). However, while the Greenland ice core temperature record and its Antarctic surrogate (GL_T_syn_hi, which is the inverse rate of change of the Antarctic temperature record; Barker et al., 2011) might be poor indicators of meridional heat transport associated with the AMOC, results from a range of climate model experiments (using models with different complexities and a variety of triggering mechanisms) suggest that changes in the strength of the AMOC can ultimately lead to the observed relationship between surface temperature changes in the north and south on millennial timescales (Schmittner et al., 2003; Liu et al., 2009; Zhang et al., 2014; Zhang et al., 2017; although this is less clear for decadal to centennial timescales; Muir & Fedorov, 2015). Accordingly, we view the record of GL_T_syn_hi as a zeroth-order proxy for anomalies in the strength of AMOC, that is, we interpret a millennial-scale warming (cooling) over Antarctica and corresponding negative (positive) value of GL_T_syn_hi to reflect a relatively weak (strong) mode of the AMOC. An equilibrium mode of AMOC (not anomalously strong or weak with respect to background conditions) would be reflected by GL_T_syn_hi remaining close to zero (Antarctica not warming or cooling on a millennial timescale) for a prolonged period such as observed during full interglacial and glacial maxima (Barker et al., 2011). We therefore infer from Figure 4 that atmospheric CO_2 changes most when the AMOC is not in equilibrium (relatively high absolute values of GL_T_syn_hi). This is in agreement with a range of carbon cycle model simulations (Ganopolski & Brovkin, 2017; Kohler et al., 2005; Marchal et al., 1998; Menviel et al., 2008; Menviel et al., 2014; Schmittner & Galbraith, 2008). Note again that while our analysis implies that the connection between ocean circulation and CO_2 has remained relatively constant, it does not address the specific mechanism involved.

3. Results

3.1. The Last 800,000 Years of Abrupt Climate Variability

Records of %NPS, %NPS_hi, and IRD/g from ODP site 983 are shown in Figure 5. The records show clear glacial-interglacial variability with higher-frequency fluctuations throughout the last 800 kyr. Wavelet decomposition of the %NPS record confirms expectations that millennial-scale variability is most pronounced during times of intermediate ice volume and transitions between states (Barker et al., 2011; Hodell et al., 2015; McManus et al., 1999; Sima et al., 2004). It could be argued that the reduction in variance in the millennial band during full glacial and interglacial conditions merely reflects saturation of the %NPS proxy during those times. However, previous interglacials rarely reflect the near-zero %NPS values characteristic of modern conditions at this site (Figures 1 and 5). In particular, interglacials before MIS 11 reveal significantly higher levels of %NPS, implying colder conditions reminiscent of the "lukewarm interglacials" observed in Antarctic and deep ocean temperature records as well that of atmospheric CO_2 (Elderfield et al., 2012; PIGS_working_group, 2016). The fact that %NPS is far from saturation during these earlier interglacials gives us confidence in our assertion that millennial-scale variability really is subdued during these periods.

3.2. Changing Atmospheric CO_2 and North Atlantic Climate Over the Past Eight Glacial Cycles

In Figure 6 we show an analysis of the relationship between changing atmospheric CO_2 and North Atlantic surface conditions over the last ~800 kyr (section 2.2). Periods of intense ice rafting *and* high %NPS_hi at ODP site 983 (i.e., anomalously cold with respect to background conditions) are dominated by increasing CO_2 (sector *X* in Figures 6a and 6b), whereas CO_2 tends to decrease during intervals of anomalous warmth *and* minimal ice rafting (sector *Y* in Figures 6a and 6b). Note that more than 75% of instances (representing discrete 200-year intervals) within sectors *X* and *Y* have positive and negative rates of dCO_2/dt, respectively. The distribution of cumulative CO_2 rise and fall with respect to surface conditions at ODP site 983 over the last 800 kyr (Figures 6c and 6d) is consistent with that observed over the last glacial cycle using either NE Atlantic SST (Martrat et al., 2007) or Greenland ice core $\delta^{18}O$ as a proxy for temperature (NGRIP_members, 2004; section 2.2 and Figure 3). Our analysis is insensitive to whether we employ the concentration of IRD (IRD/g) or the accumulation rate (Figure 6c) because of the large range (6 orders of magnitude) in IRD delivery to the site, which hugely outweighs the effects of changing bulk sedimentation rate

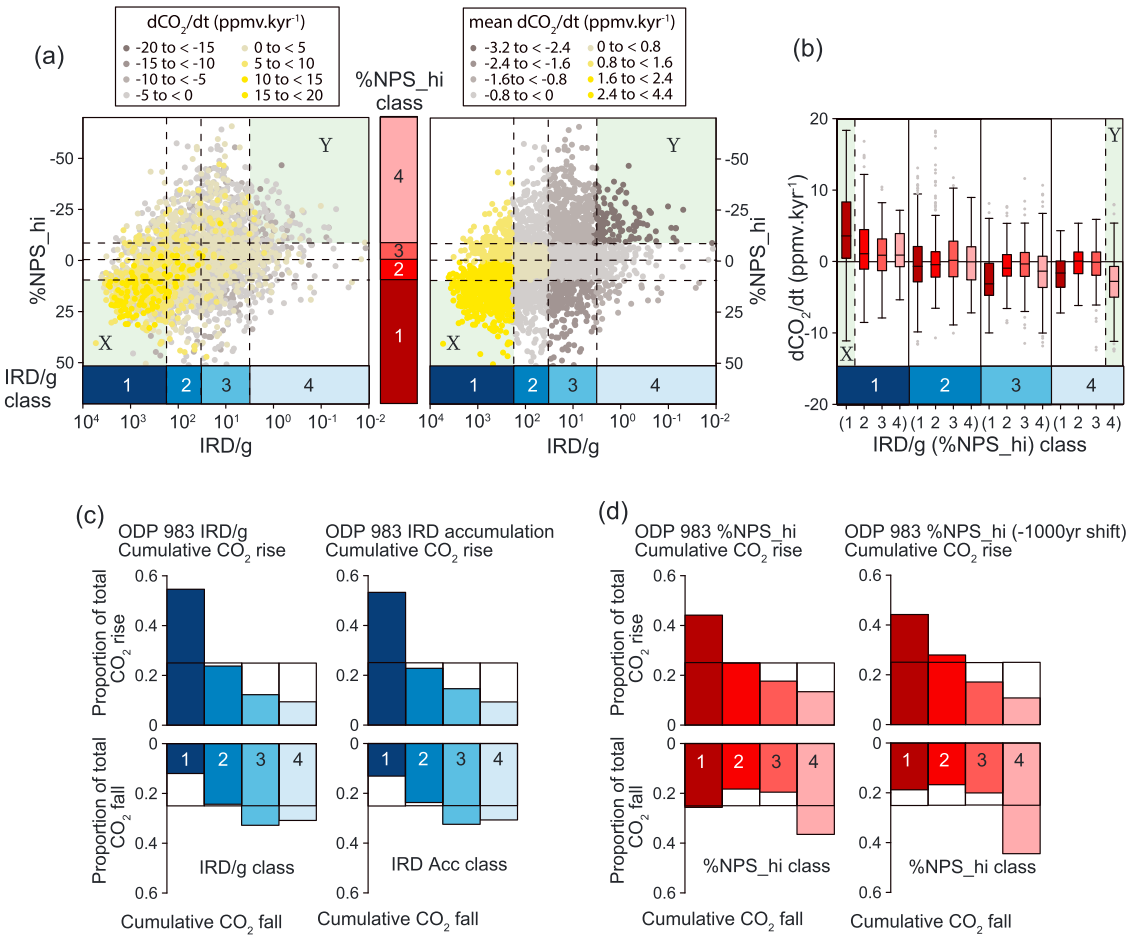

Figure 6. Changing CO_2 versus surface conditions across the North Atlantic region over the past 800 kyr. (a) %NPS_hi versus IRD/g from ODP 983, color coded by contemporaneous rate of CO_2 change (left) or mean dCO_2/dt for each sector (right). Each dot represents a discrete 200-year interval. Sector *X* (*Y*) represents the coldest (warmest) and iciest (least icy) intervals. (b) Box plots showing the distribution of dCO_2/dt for each sector in (a). (c, left) Distribution of cumulative CO_2 rise (upper) and fall (lower) across IRD/g classes as defined in (a) over the past 800 kyr. (Right) same as left but using IRD accumulation rate instead of IRD/g. (d, left) Distribution of cumulative CO_2 rise (upper) and fall (lower) across %NPS_hi classes as defined in (a) over the past 800 kyr. (Right) same as left but with %NPS_hi shifted by −1,000 year (see text). For all parts Class 1 represents the coldest (or iciest) quartile (25% of the time) and Class 4 the warmest (or least icy). IRD = ice rafted debris.

on the concentration of IRD. By analogy to the observed relationship between changes in ocean circulation and surface conditions in the North Atlantic region during the last glacial and deglacial periods (Figure 2), we therefore conclude that the relationship between changing atmospheric CO_2 and ocean circulation as observed over the last glacial cycle (Ahn & Brook, 2008; Deaney et al., 2017; Henry et al., 2016; Marcott et al., 2014) has been relatively invariant over the past 800 kyr, as also suggested by the analysis shown in Figure 4.

While our analysis confirms that a major proportion of CO_2 rise over the past 800 kyr coincided with cold, icy conditions across the North Atlantic, it does not negate the observation that CO_2 does not always rise when the North Atlantic is cold (Ahn & Brook, 2014). This is clear from the many instances where CO_2 does not change or even decreases while cold conditions prevail (Figures 3 and 6). In fact from Figures 6a and 6b it can be seen that anomalously cold intervals at ODP site 983 (%NPS_hi Class 1) which also have low relative concentrations of IRD (IRD Classes 3 and 4) display a bias toward decreasing CO_2. The result is that ~25% of cumulative CO_2 fall over the past 800 kyr coincides with the coldest quartile at this site (Figure 6d), which is somewhat at odds with our analysis of the equivalent relationship between dCO_2/dt and NE Atlantic SST or Greenland $\delta^{18}O$ (Figure 3). Previously, (Barker et al., 2015) we showed that surface cooling at site 983 can occur hundreds to thousands of years before the transition to stadial conditions as recorded over

Greenland and may therefore occur while atmospheric CO_2 is decreasing during a warm Greenland interstadial (thus, some of an interstadial decrease in CO_2 effectively "leaks" into a cold interval at site 983). This would explain why the seemingly anomalous intervals of decreasing CO_2 correspond to intervals of reduced IRD (i.e., during interstadials if defined as periods with low IRD). The effect can be demonstrated by systematically shifting the age assignments of the 983 %NPS_hi record toward younger ages (Figure 6d). Doing so effectively shifts the cooling transitions so they no longer intersect (to such an extent) with intervals of decreasing CO_2 (i.e., they occur later with respect to the change in CO_2).

Our age model for ODP site 983 is derived by tuning to the ice core record on the AICC2012 age model. Therefore, we need to be concerned about the relative errors between our age model and AICC2012 for our comparisons to the record of atmospheric CO_2. Uncertainties in the relative age models of 983 (as determined here) and the CO_2 record derive partly from the precision of tuning between abrupt transitions (of the order of a few hundred years for individual tie points, Barker et al., 2011) and also from the possibility of choosing the wrong transitions, which is difficult to quantify. We therefore assess the impact of potential uncertainties in the age model by repeating the analyses with systematic shifts in the age assignments of the 983 records (Figure S5). By applying a systematic shift to the whole record, we are greatly exaggerating the likely effect of true errors since we expect a distribution of errors with a mean approximating zero along the 800-kyr length of the records. However, even when shifting the age model by 1,000 years in either direction, the distribution of cumulative CO_2 change versus IRD/g is minimally affected. The largest impact is on the cumulative fall in CO_2 with respect to %NPS_hi (as described above). The relative insensitivity of our analyses to large changes in age assignment is to some extent due to the 2-kyr presmoothing of the CO_2 record before differentiating. This has the effect of "spreading" the influence of intervals of changing CO_2 beyond their actual limits, which flattens the distribution across classes and also buffers against age model error.

We also compare our age model with that produced for the same core by Lisiecki and Raymo (2005) as part of the LR04 benthic foraminiferal $\delta^{18}O$ stack (Figure S5). Note that we did not produce the age model used in this comparison. Use of the LR04 age model necessarily alters the calculated distribution of cumulative CO_2 rise and fall because many millennial-scale oscillations will be completely misaligned. However, it does not affect the general relationship observed when using the tuned age model. This probably reflects the fact that the timing of glacial terminations within LR04 is very similar to that implied by the AICC2012 ice core age model (note benthic $\delta^{18}O$ records in Figure 7); that is, the major terminal ice rafting events and corresponding shifts in atmospheric CO_2 are aligned irrespective of the age model employed.

3.3. Glacial Terminations at ODP Site 983

Glacial terminations at ODP site 983 are characterized by pulses of ice rafting followed by an abrupt warming—a shift from high to low %NPS (Figures 5 and 7). We interpret these phenomena to reflect early deglacial ice sheet wasting and related freshwater release (in the form of melting icebergs) to the North Atlantic while cold conditions prevail. Once ice rafting ceases, the abrupt warming reflects northward migration of the polar front (Barker et al., 2015; Zahn, 1994) (Figure 1). Our results are consistent with previous studies suggesting a ubiquitous link between abrupt climate shifts and deglaciation (Barker et al., 2011; Cheng et al., 2009; Cheng et al., 2016; Venz et al., 1999), and by analogy with the last two terminations, where direct reconstructions of ocean circulation exist (Böhm et al., 2015; Deaney et al., 2017; McManus et al., 2004; Roberts et al., 2010), we infer that terminal ice rafting events in general are associated with a weakened and or shallow mode of AMOC [see also Venz et al., 1999] with the subsequent shift to warm, ice-free conditions reflecting recovery of the AMOC and in particular an increased flow of warm Atlantic surface waters into the Norwegian Sea (Lehman & Keigwin, 1992) and corresponding strengthening of the so-called Nordic heat pump (Imbrie et al., 1992). The term Nordic heat pump describes the transfer of heat across the Greenland-Scotland Ridge via warm surface Atlantic waters entering the Nordic Seas and their return to the deep NE Atlantic as dense overflows across the Greenland-Scotland ridge (Dickson & Brown, 1994; Imbrie et al., 1992). A strong Nordic heat pump is characteristic of interglacial conditions (Figure 1; Imbrie et al., 1992; Berger & Jansen, 1994), whereas a southward shift in the mean latitude of deep water formation (as thought to accompany full glacial conditions; Weber et al., 2007) would indicate a relative strengthening of the so-called boreal heat pump (characterized by open-ocean convection in the boreal Atlantic) at the expense of the Nordic heat pump (Imbrie et al., 1992; Figure 1). Higher bulk sediment

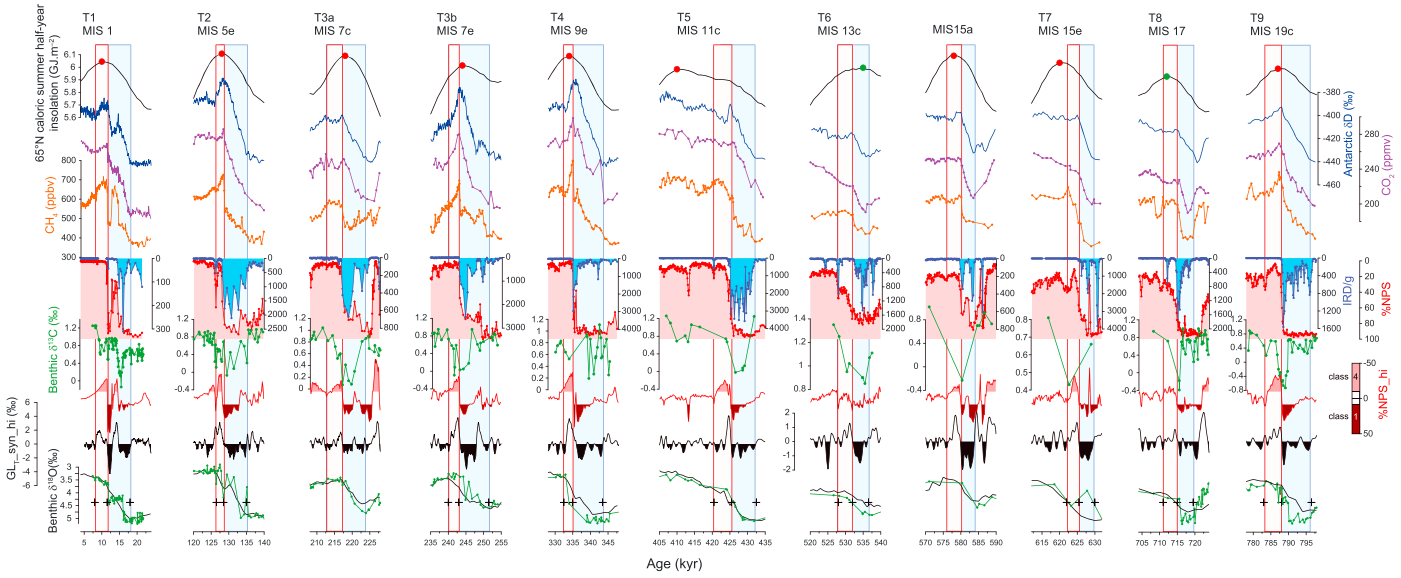

Figure 7. Glacial terminations of the last 800 kyr. All panels from top to bottom: Integrated summer insolation (Tzedakis et al., 2017; colored circles as in Figure 5), Antarctic temperature proxy (δD; Jouzel et al., 2007), atmospheric CO_2 (Bereiter et al., 2015), atmospheric CH_4 (Loulergue et al., 2008), ice rafted debris/g, %NPS, benthic foraminiferal $\delta^{13}C$ (Channell et al., 1997; Raymo et al., 2004) and %NPS_hi all from ODP 983, GL_T_syn_hi (Barker et al., 2011), benthic $\delta^{18}O$ from ODP 983 (Channell et al., 1997; Raymo et al., 2004) (green), and the LR04 $\delta^{18}O$ stack on its independent age model (Lisiecki & Raymo, 2005) (black). Blue boxes represent main deglacial phase of ice rafting until start of interglacial conditions according to definition 1 (see text). Pink boxes represent intervals of anomalous surface warmth (low %NPS_hi) and strong Atlantic Meridional Overturning Circulation (high GL_T_syn_hi) prior to the start of equilibrium interglacial conditions according to definition 2 (see text). Records from nearby core RAPiD-17-5P (Thornalley et al., 2010) are used instead of those from ODP 983 over the interval 7.5-21.3 ka due to the lower quality benthic $\delta^{13}C$ record from 983 across this interval.

accumulation rates observed at ODP site 983 during interglacials (Barker et al., 2015; Lisiecki & Raymo, 2005) provide supporting evidence for stronger Iceland-Scotland overflows (and by extension a stronger Nordic heat pump) during these intervals.

4. Discussion

In order to make comparisons among previous interglacials, it is necessary to define the beginning and end of these periods (PIGS_working_group, 2016; Ruddiman et al., 2016; Tzedakis et al., 2012; Tzedakis et al., 2017). In particular, the occurrence of millennial-scale features associated with the onset of several past interglacials, for example, within the Antarctic ice core records of temperature and greenhouse gasses (including CO_2), gives rise to considerable ambiguity in defining the onset of interglacial conditions (Masson-Delmotte et al., 2010; PIGS_working_group, 2016). In the following discussion we consider two alternative definitions for the start of interglacial conditions. The first of these (definition 1) was introduced by Tzedakis et al. (2012) and is defined as the last significant bipolar-seesaw oscillation (Stocker & Johnsen, 2003) associated with glacial termination. This corresponds to the end of the Younger-Dryas during T1 and the end of Heinrich Event 11 during T2 (Tzedakis et al., 2012). In Figure 7 this definition is represented by the transition from blue to pink shaded box for each deglaciation of the last 800 kyr. According to our age modeling approach, abrupt deglacial warming at ODP site 983 (implied by strongly decreasing %NPS and the end of major ice rafting) is aligned with the abrupt warming (and strengthening of AMOC) implied by GL_T_syn_hi (section 2.3). Hence, warm "interglacial" conditions at ODP site 983 begin in parallel with the onset of interglacial climate according to Definition 1. On the other hand there are several lines of evidence which suggest that the residual effects of deglaciation can last for thousands of years beyond this point, which we explore below.

4.1. Delayed Equilibration of Ocean Circulation During an Interglacial

Venz et al. (1999) noted that deglacial minima in a record of benthic foraminiferal $\delta^{13}C$ obtained from ODP site 982 (close by site 983) persisted well beyond the end of terminal ice rafting events (recorded at the same

site) for several previous interglacials. They interpreted this to reflect a delayed recovery of full interglacial-like circulation beyond the start of some interglacials. We observe the same behavior at ODP site 983 (Figure 7); deglacial minima in benthic $\delta^{13}C$ can persist for thousands of years beyond the end of ice rafting and abrupt warming at this site. Although benthic foraminiferal $\delta^{13}C$ is not a conservative tracer for circulation (being sensitive to changes in biology and end-member variability), there are other lines of evidence supporting the assertion that ocean circulation may not recover to its full (quasi-equilibrium) interglacial mode for thousands of years beyond termination. Previous studies across T2, using sedimentary grain size as a proxy for the vigor of one of the main deep water currents crossing the Iceland-Scotland Ridge (Iceland-Scotland Overflow Water, ISOW), have concluded that the production and / or density of deep waters formed in the Nordic Seas (a critical component of the modern Nordic heat pump) during the earliest part of the last interglacial period was subdued by continued melting of proximal ice sheets (Deaney et al., 2017; Hodell et al., 2009). A similar case has been made for the delayed recovery of a modern-like AMOC during the early Holocene (Thornalley et al., 2010; Thornalley et al., 2013).

Masson-Delmotte et al. (2010) suggested that early interglacial maxima observed in the Antarctic ice core temperature record are caused by "transient heat transport redistribution comparable with glacial north-south seesaw abrupt climatic changes." Indeed, the millennial-scale cooling observed across Antarctica as these early interglacial maxima subside gives rise to positive anomalies in the derived record of GL_T_syn_hi (implying an anomalously strong mode of AMOC according to our reasoning) that persist for approximately the same duration as the anomalous conditions implied by the record of benthic $\delta^{13}C$ from site 983 (Figure 7). But how can these records be reconciled? The records of benthic $\delta^{13}C$ and sortable silt seem to imply a "weaker" mode of the Nordic heat pump (at least with respect to full interglacial conditions) during the early part of some interglacials, while GL_T_syn_hi implies a stronger mode of AMOC. One possibility is that reduced overflow across the Iceland-Scotland ridge (i.e., ISOW) was (more than) compensated by increased transport of deep waters across the Greenland-Iceland ridge (i.e., Denmark Strait Overflow Water, resulting in a net strengthening of the Nordic heat pump on its deglacial recovery. On the other hand millennial-scale cooling or warming across Antarctica, in response to changes in the AMOC, is most likely insensitive to the location of deep water formation in the North Atlantic. Thus, we need only invoke a net strengthening of the North Atlantic heat pump in a broad sense (the combined Nordic and boreal heat pumps) with respect to equilibrium interglacial conditions in order to reconcile these disparate observations. The potential importance of deep water formation in the subpolar open ocean (i.e., the boreal heat pump) during deglaciation and the onset of abrupt warming events has been suggested by previous modeling studies (e.g., Barker et al., 2010; Knorr & Lohmann, 2007).

Building on the model of Broecker and Denton (1989), Imbrie et al. (1992, 1993) proposed that the transition from glacial to interglacial state involves a shift from a "one-pump" to a "two-pump" mode. In their model deep water formation in the glacial North Atlantic is limited to the south of Iceland, reflecting a weaker Nordic heat pump and stronger-than-modern boreal heat pump (the "one-pump" mode) with total overturning reduced relative to modern conditions (this inference is qualitatively supported by several model simulations of the glacial AMOC; Weber et al., 2007). During termination, recovery of the Nordic heat pump occurs while the boreal heat pump is still strong, giving rise to a transient maximum in Atlantic overturning even if the Nordic heat pump does not initially recover to its full interglacial strength (see Figure 4 in Imbrie et al., 1992). The evidence outlined above seems to provide qualitative support for such a scenario; the shift from negative to positive GL_T_syn_hi implies (by our reasoning) a strengthening of AMOC, and if our alignment strategy is correct, this is paired with a strong warming at the site of ODP 983, which would represent a northerly shift of the polar front and implied strengthening of the Nordic heat pump (Imbrie et al., 1992; Imbrie et al., 1993; Lehman & Keigwin, 1992). This transition is followed by a period of anomalously strong AMOC (according to GL_T_syn_hi), which may be accommodated by a stronger-than-modern boreal heat pump even if the Nordic heat pump is not yet up to full interglacial strength (as indicated by the benthic $\delta^{13}C$ and sortable silt data).

Several outstanding issues arise from this discussion, which should be addressed in future studies undertaking more detailed investigations into regional patterns. For example, how do the individual components of AMOC (i.e., ISOW, Denmark Straits Overflow Water, and Labrador Sea Water, LSW) contribute to early interglacial changes in AMOC and do they do so in a consistent manner as appears the case for the

combined AMOC (as proxied by our records from ODP Site 983)? What is the precise mechanism driving the anomalously strong AMOC as proposed during early interglacial time and how is it related to forcing such as insolation, remnant ice-sheets or possible Southern Ocean processes influencing rates of upwelling from the deep ocean?

4.2. Comparing Apples and Oranges: When Is an Interglacial Not an Interglacial?

In our records from ODP site 983 we observe transient maxima in %NPS_hi, which resemble the early interglacial maxima in GL_T_syn_hi, following the end of major deglacial ice rafting events (Figure 7). We note that typical interglacial values of %NPS prior to MIS 1 are greater than zero, and as such we maintain that this result is not an artifact of proxy saturation. Our analysis suggests that conditions in the NE Atlantic can remain anomalously warm with respect to background conditions for thousands of years after the onset of interglacial conditions according to Definition 1. We propose that this reflects the inferred net strengthening of the AMOC (relative to equilibrium interglacial conditions) directly following its deglacial recovery, providing excess heat to the high-latitude surface North Atlantic and aiding in the completion of Northern Hemisphere deglaciation (Imbrie et al., 1992; Imbrie et al., 1993; Lehman & Keigwin, 1992). We note that some early interglacial values of %NPS, which we define as anomalous, are very similar in absolute terms to later values that are not considered anomalous. Again, this could be used to argue that the transient early interglacial maxima in %NPS_hi are simply artifacts of our analysis. On the other hand where we have reconstructions of "regional" surface temperature evolution, for example, across T1 and T2, (Hoffman et al., 2017; Shakun et al., 2012), we see that the abrupt warming implied by our record of %NPS does indeed occur thousands of years before the end of gradual North Atlantic or Northern Hemisphere warming (Figure S6) and should thus be considered as anomalous. The local surface temperature evolution at the site of ODP 983 reflects both regional ("background") temperature variability of Atlantic surface water masses, superimposed by changes in the transport and mixing of those water masses, and although regional reconstructions must also contain both of these signals, the northerly position of ODP site 983 makes it particularly sensitive to changes in circulation.

Given the different lines of evidence for anomalous (nonequilibrium) conditions lasting beyond the start of an interglacial according to Definition 1, we propose a second definition (Definition 2) for the onset of quasi-equilibrium interglacial conditions that coincide with the end of this anomalous phase as expressed by %NPS_hi, benthic $\delta^{13}C$, and GL_T_syn_hi (the end of the pink box in Figure 7). In several cases this definition could be extended to encompass secondary features but we limit our description to include only the major features. Note that our aim is not to reinvent the definition of an interglacial but rather to highlight the complexities introduced by nonequilibrium conditions when making comparisons among different interglacials. In this respect we are reiterating earlier warnings (e.g., Masson-Delmotte et al., 2010; PIGS_working_group, 2016). Below we investigate the implications of this complexity for investigations into the interglacial evolution of atmospheric CO_2.

In Figure S7 we plot the coevolution of benthic $\delta^{18}O$ (a crude proxy for global ice volume) versus atmospheric CO_2 for the last eight glacial cycles. Although the records are on independent age models (LR04 versus AICC2012), a deglacial lead of increasing CO_2 ahead of decreasing ice volume is discernable for the majority of cases (note the exceptions T6 and T8 will be discussed later). This was demonstrated with greater precision in a study by Shackleton et al. (2000) and conveniently conveys the importance of rising CO_2 as a critical ingredient in the deglacial process (Broecker & Denton, 1989; Imbrie et al., 1993; Shakun et al., 2012). The colored symbols in Figures 8a and 8b) represent the coevolution of benthic $\delta^{18}O$ and CO_2 across the last nine glacial terminations using the first and second definitions, respectively, for the onset of interglacial conditions (i.e., across the blue or blue and pink boxes combined in Figure 7). It is unsurprising that use of Definition 2 encompasses a more complete transition with respect to benthic $\delta^{18}O$ as compared with Definition 1; on orbital timescales ice volume typically responds later than other climatic indicators (Shackleton, 2000), for example, during the most recent deglaciation sea level continued to rise until at least 8 ka, well beyond the conventional start of the Holocene interglacial (Smith et al., 2011).

On the other hand, the main phase of deglacial CO_2 rise typically occurs prior to the onset of interglacial conditions irrespective of which definition is used, that is, most of the rise in CO_2 takes place within the blue boxes in Figure 7. Of particular relevance though are several instances (T1, T3b, T4, ans T9) where use of

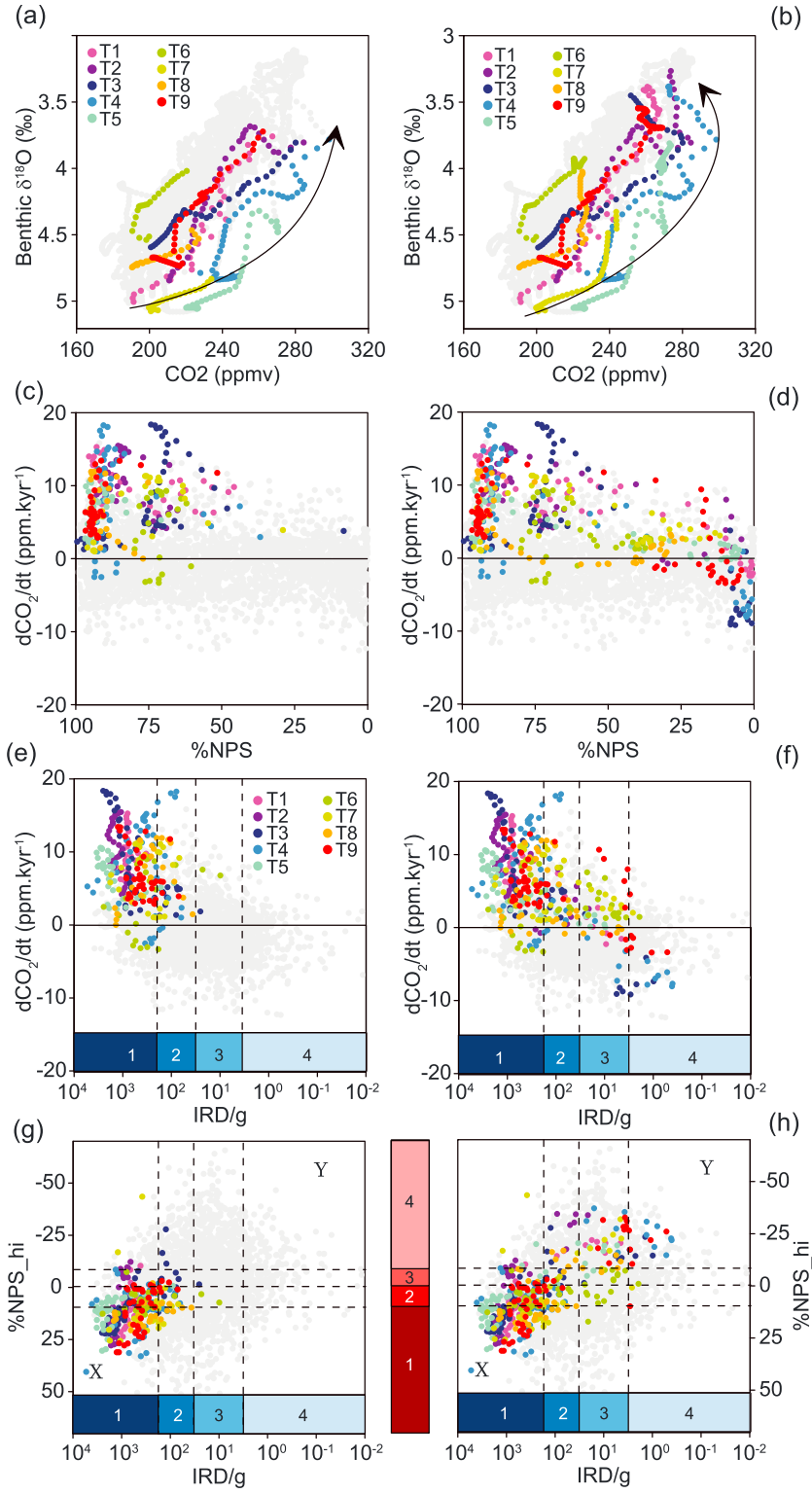

Figure 8. Individual deglacial transitions according to definitions 1 (left-hand panels) and 2 (right-hand panels) for the start of interglacial conditions. (a, b) Benthic $\delta^{18}O$ (Lisiecki & Raymo, 2005) versus atmospheric CO_2 (Bereiter et al., 2015; arrow is schematic representation of deglacial trend; see also Figure S6). (c, d) dCO_2/dt versus %NPS from ODP 983. (e, f) dCO_2/dt versus IRD/g. (g, h) %NPS_hi versus IRD/g (partitions and labels as in Figure 6). T1-9 are terminations 1 to 9 with color coding the same in each panel. IRD = ice rafted debris.

Definition 2 incorporates an interval of decreasing CO_2 prior to the implied onset of equilibrium interglacial conditions (Figure 8b). These phases of decreasing CO_2 correspond to particularly warm (low %NPS) and relatively ice-free (low IRD/g) conditions at the site of ODP 983 (Figures 8d and 8f). In fact, several terminations (including T3b, T4, and T9; Figure 8h) extend into sector *Y* in Figures 6a and 6b; conditions that are typically associated with decreasing atmospheric CO_2. Notably, terminations T3b, T4, and T9 reveal higher rates of CO_2 decrease during their early "nonequilibrium" interglacial sections than any other deglaciation of the past 800 kyr. These terminations also correspond to MIS 7, 9, and 19, which were identified by Ruddiman et al. (2016) as those interglacials most consistently associated with a decreasing trend in atmospheric CO_2. We believe that our observation of a systematic link between changing CO_2 and nonequilibrium oceanic conditions during the early phase of several previous interglacials provides a strong basis for concluding that this link is causal, that is, that an early interglacial decrease in atmospheric CO_2 is most likely a direct consequence of a nonequilibrium ocean state. Such an inference is in line with transient carbon cycle modeling studies which consistently imply that CO_2 will change whenever ocean circulation is not in equilibrium (Ganopolski & Brovkin, 2017; Kohler et al., 2005; Marchal et al., 1998; Menviel et al., 2008; Menviel et al., 2014; Schmittner & Galbraith, 2008).

We therefore suggest that the early interglacial intervals we identify as anomalous (Figures 5 and 7) should not be counted in any survey of interglacial trends where quasi-equilibrium conditions may be assumed; for these purposes such intervals should be considered as a part of the deglacial process. For example, the highest interglacial values of CO_2 during MIS 5, 7, 9, and 19 occur within the intervals we identify as anomalous (the pink boxes in Figures 5 and 7). If these intervals were not included in the analysis of interglacial CO_2, it is unclear that such a consistent decreasing trend in CO_2 would be identified for these particular interglacials. Thus, while we are not commenting on the overall conclusions of Ruddiman et al. (2016), our findings do suggest that some reevaluation may be required. We stress again that we are not trying to redefine what an interglacial is and we do not consider Definition 2 as a "better" definition of when an interglacial begins. Here we are concerned with the legacy of deglacial instabilities, which we suggest can last for thousands of years after the beginning of an interglacial as traditionally defined.

As to why some interglacials experience more pronounced overshoots in CO_2 than others, we concur with earlier studies (Deaney et al., 2017; Ganopolski & Brovkin, 2017) which suggest that this might be related to the timing of AMOC recovery with respect to deglaciation; If recovery occurs midway through the termination (e.g., with the Bølling-Allerød during T1), then we might expect a smaller overshoot than for a termination where AMOC recovery occurs only toward the end (e.g., T2). The case of T3b is an interesting one (Figure 7); the records of %NPS_hi and GL_T_syn suggest that the AMOC might have made an early recovery (albeit a partial one considering the small decrease in %NPS) ~250 ka, and yet we observe a large overshoot in CO_2 at the end of termination ~243 ka. Recovery of the AMOC during deglaciation may occur with the cessation of freshwater release across the North Atlantic (Ganopolski & Brovkin, 2017; Liu et al., 2009) or in response to more gradual global warming in which case the addition of freshwater may still act to delay resumption (Knorr & Lohmann, 2007). Future studies should focus on the interplay between these parameters when considering individual terminations.

4.3. Protracted Terminations: T6, T8, (and T5?)

Tzedakis et al. (2017) formulated a simple rule for predicting the occurrence of interglacials as a function of integrated northern summer insolation. Their predictions provide insight into some of the atypical behavior we observe associated with a number of terminations. For example, the warming transitions (shift from high to low %NPS) following the major deglacial pulses of ice rafting associated with T6 (leading to MIS 13; Figure 7) and T8 (leading to MIS 17) are not particularly abrupt or pronounced. In fact, these terminations end with the least anomalous values of %NPS_hi (out of all the deglacial transitions covered here) and are followed by further pulses of ice rafting while warming continues. Hence, we label these transitions protracted terminations. We note that both T6 and T8 are associated with insolation peaks that do not pass the Tzedakis test (i.e., they do not cross the threshold for producing an interglacial state according to that study; Figure 5), even though subsequent peaks allow for inclusion of MIS 13 and MIS 17 within the set of Late Pleistocene interglacials. We note also that the cycles of benthic $\delta^{18}O$ versus atmospheric CO_2 from MIS 15 to 13 and from MIS 19 to 17 (Figure S7) do not show the same apparent hysteresis as other cycles. The deglacial rise in CO_2 across T6 (and to a lesser extent across T8) does not lead the initial decrease in $\delta^{18}O$ (ice

volume) and CO_2 continues to increase gradually throughout deglaciation. The formulation presented by Tzedakis et al. (2017) utilizes a discount applied to the threshold required to generate an interglacial, which depends on the time since the threshold was last crossed. Implicit in their argument is the existence of a component within the climate system that is capable of storing the potential "energy" (or equivalent) required to amplify a modest increase in summer insolation and produce a glacial termination. Crucially, for T6 and T8, this component must not lose its (full) potential during the initial phase of deglaciation (which occurs much earlier than the insolation peak that eventually passes the Tzedakis test). Our results suggest that T6 and T8 were atypical in that changes across them were less pronounced than other terminations. We note that for T8, atmospheric CO_2 continued to rise (albeit only on average) until the threshold was crossed, but T6 was more complicated. We also note that the insolation peak associated with T5 (leading into MIS 11) comprises two precession peaks, and it is only the second of these (in combination with high obliquity) that exceeds the threshold for an interglacial. Perhaps this could help to explain why the transition from MIS 12 to MIS 11 also appears somewhat protracted (Figure 5) as described by Rohling et al. (2010).

4.4. The "Nonuniqueness" of Heinrich Events

Heinrich (1988) and Bond et al. (1992) described a series of detrital layers deposited across the midlatitude North Atlantic. These layers of IRD were proposed to reflect episodic collapses of the Laurentide ice sheet ("Heinrich events") with icebergs being discharged through the Hudson Strait providing meltwater to large portions of the surface North Atlantic. The longest (NGRIP_members, 2004) and coldest (Martrat et al., 2007; Shackleton et al., 2000) stadial events recorded across the North Atlantic region during MIS 3 were associated with H-events, and these have been termed Heinrich stadials (Barker et al., 2009; Skinner & Elderfield, 2007). The large volume of freshwater release associated with H-events (Hemming, 2004) is thought to have affected ocean circulation, and empirical evidence suggests that H-stadials were associated with particularly strong perturbations of the AMOC as compared with non-H stadials (Henry et al., 2016; Piotrowski et al., 2005). The H-stadials of MIS 3 were also associated with much larger increases in atmospheric CO_2 than the smaller non-H stadials (Ahn & Brook, 2008; Ahn & Brook, 2014). Thus, Heinrich events themselves have become synonymous with extreme perturbations of the AMOC and rising atmospheric CO_2. On the other hand it is not clear whether H-events were the primary cause of such perturbations (Alvarez-Solas et al., 2013; Barker et al., 2015; Bond & Lotti, 1995; Shaffer et al., 2004). Furthermore, a number of studies provide evidence that Heinrich events in a strict sense (i.e., sourced from Hudson Strait) first appeared around 640 ka (Hodell et al., 2008; Naafs et al., 2011) but we do not observe any systematic change in the relationship between surface conditions and changing atmospheric CO_2 across this interval (Figure S8), suggesting that the observed correlation between Heinrich events and millennial-scale changes in atmospheric CO_2 during the last glacial cycle does not necessarily reflect an exclusive causal link. We propose therefore that the massive Hudson Strait ice discharge events were not unique in terms of their potential impact on ocean circulation and atmospheric CO_2, allowing for the possibility that another source of freshwater or alternative mechanism might play an important role.

5. Conclusions

We have presented continuous proxy records of NE Atlantic surface conditions spanning the past 800 kyr, encompassing eight glacial cycles and nine glacial terminations. Our records confirm that the occurrence of millennial-scale variability throughout this period was most pronounced during times of intermediate ice volume and transitions between glacial and interglacial states. Our results reveal a link between surface ocean conditions and changes in atmospheric CO_2 that is consistent with independent observations and reconstructions over the last glacial cycle, and we therefore infer that the hypothesized mechanistic link between ocean circulation and CO_2 (with CO_2 rising on a millennial timescale when Atlantic circulation is in a weakened state and vice versa) has been maintained throughout the last 800 kyr.

According to our reconstructions, glacial terminations are characterized by a prolonged interval of cold, icy conditions across the high-latitude North Atlantic during which atmospheric CO_2 rises and (by our reasoning) the AMOC is in a weakened state. Subsequent and abrupt warming occurs with the end of iceberg discharge and is followed by an interval of anomalous warmth during which CO_2 may decrease again before reaching its equilibrium interglacial concentration. We interpret this sequence of events to reflect the recovery and amplification of AMOC during early interglacial times when we infer there to be a stronger-than-

modern boreal heat pump in combination with a strong, or strengthening, Nordic heat pump. We therefore suggest that the evolution of atmospheric CO_2 during these periods reflects nonequilibrium conditions (i.e., the climate system has not yet reequilibrated following deglaciation) and should not be considered within comparisons among interglacials. A number of deglaciations (in particular Terminations 6 and 8 and potentially T5) do not follow the typical trend, with less pronounced warming and multiple phases of ice rafting. These deglaciations also experienced weaker insolation forcing than is considered requisite to give rise to interglacial conditions, and we label these as protracted terminations. Finally, we note that the observed relationship between surface ocean conditions and changing CO_2 did not change with the onset of Heinrich events sourced from the Hudson Strait ~640 ka. We therefore conclude that Heinrich events were not unique in terms of their potential impact on ocean circulation and atmospheric CO_2, sustaining the question as to the precise drivers of large-scale perturbations of the AMOC and corresponding variations in CO_2.

Acknowledgments
We thank the Editor, Luke Skinner, and two anonymous reviewers for their careful and constructive evaluations of our study. This research used samples provided by the Integrated Ocean Drilling Program (IODP). We acknowledge support from U.K. NERC (Grants NE/J008133/1, NE/P000878/1, and NE/L006405/1). Author contributions are as follows: S. B. designed project and analyzed data sets; S. C., S. L., and D. N. performed all laboratory work. All authors contributed to writing the paper. The authors declare no competing interests. All data presented here are available in the supporting information and online in the PANGAEA data repository (https://doi.pangaea.de/10.1594/PANGAEA.904398).

References

Ahn, J., & Brook, E. J. (2008). Atmospheric CO_2 and climate on millennial time scales during the last glacial period. *Science*, *322*(5898), 83–85. https://doi.org/10.1126/science.1160832

Ahn, J., & Brook, E. J. (2014). Siple Dome ice reveals two modes of millennial CO_2 change during the last ice age. *Nature Communications*, *5*(1), 3723. https://doi.org/10.1038/ncomms4723

Alley, R. B., Brook, E. J., & Anandakrishnan, S. (2002). A northern lead in the orbital band: North-south phasing of Ice-Age events. *Quaternary Science Reviews*, *21*(1-3), 431–441. https://doi.org/10.1016/S0277-3791(01)00072-5

Alvarez-Solas, J., Robinson, A., Montoya, M., & Ritz, C. (2013). Iceberg discharges of the last glacial period driven by oceanic circulation changes. *Proceedings of the National Academy of Sciences of the United States of America*, *110*(41), 16,350–16,354. https://doi.org/10.1073/pnas.1306622110

Anderson, R. F., Ali, S., Bradtmiller, L. I., Nielsen, S. H. H., Fleisher, M. Q., Anderson, B. E., & Burckle, L. H. (2009). Wind-driven upwelling in the Southern Ocean and the deglacial rise in atmospheric CO_2. *Science*, *323*(5920), 1443–1448. https://doi.org/10.1126/science.1167441

Barker, S., Chen, J., Gong, X., Jonkers, L., Knorr, G., & Thornalley, D. (2015). Icebergs not the trigger for North Atlantic cold events. *Nature*, *520*(7547), 333–336. https://doi.org/10.1038/nature14330

Barker, S., Diz, P., Vautravers, M. J., Pike, J., Knorr, G., Hall, I. R., & Broecker, W. S. (2009). Interhemispheric Atlantic seesaw response during the last deglaciation. *Nature*, *457*(7233), 1097–1102. https://doi.org/10.1038/nature07770

Barker, S., Knorr, G., Edwards, R. L., Parrenin, F., Putnam, A. E., Skinner, L. C., et al. (2011). 800,000 years of abrupt climate variability. *Science*, *334*(6054), 347–351. https://doi.org/10.1126/science.1203580

Barker, S., Knorr, G., Vautravers, M., Diz, P., & Skinner, L. C. (2010). Extreme deepening of the Atlantic overturning circulation during deglaciation. *Nature Geoscience*, *3*, 567–571. https://doi.org/10.1038/NGEO1921

Bazin, L., Landais, A., Lemieux-Dudon, B., Kele, H. T. M., Veres, D., Parrenin, F., et al. (2013). An optimized multi-proxy, multi-site Antarctic ice and gas orbital chronology (AICC2012): 120-800 ka. *Climate of the Past*, *9*(4), 1715–1731. https://doi.org/10.5194/cp-9-1715-2013

Bereiter, B., Eggleston, S., Schmitt, J., Nehrbass-Ahles, C., Stocker, T. F., Fischer, H., et al. (2015). Revision of the EPICA Dome C CO_2 record from 800 to 600 kyr before present. *Geophysical Research Letters*, *42*, 542–549. https://doi.org/10.1002/2014GL061957

Berger, W. H., & Jansen, E. (1994). *Mid-pleistocene climate shift-the Nansen connection, The polar oceans and their role in shaping the global environment*, *Geophysical Monograph Series* (pp. 295–311).

Böhm, E., Lippold, J., Gutjahr, M., Frank, M., Blaser, P., Antz, B., et al. (2015). Strong and deep Atlantic meridional overturning circulation during the last glacial cycle. *Nature*, *517*(7532), 73–76. https://doi.org/10.1038/nature14059

Bond, G., Heinrich, H., Broecker, W., Labeyrie, L., McManus, J., Andrews, J., et al. (1992). Evidence for massive discharges of icebergs into the north Atlantic Ocean during the Last Glacial Period. *Nature*, *360*(6401), 245–249. https://doi.org/10.1038/360245a0

Bond, G. C., & Lotti, R. (1995). Iceberg discharges into the North-Atlantic on millennial time scales during the last glaciation. *Science*, *267*(5200), 1005–1010. https://doi.org/10.1126/science.267.5200.1005

Broecker, W. S., & Denton, G. H. (1989). The role of ocean-atmosphere reorganizations in glacial cycles. *Geochimica et Cosmochimica Acta*, *53*(10), 2465–2501. https://doi.org/10.1016/0016-7037(89)90123-3

Broecker, W. S., Lynch-Stieglitz, J., Clark, E., Hajdas, I., & Bonani, G. (2001). What caused the atmosphere's CO_2 content to rise during the last 8000 years? *Geochemistry Geophysics Geosystems*, *2*, U1–U13.

Broecker, W. S., & van Donk, J. (1970). Insolation changes, ice volumes and the O^{18} in deep-sea cores. *Reviews of Geophysics and Space Physics*, *8*(1), 169–198. https://doi.org/10.1029/RG008i001p00169

Caesar, L., Rahmstorf, S., Robinson, A., Feulner, G., & Saba, V. (2018). Observed fingerprint of a weakening Atlantic Ocean overturning circulation. *Nature*, *556*(7700), 191–196. https://doi.org/10.1038/s41586-018-0006-5

Channell, J. E. T., Hodell, D. A., & Lehman, B. (1997). Relative geomagnetic paleointensity and delta O-18 at ODP Site 983 (Gardar Drift, North Atlantic) since 350 ka. *Earth and Planetary Science Letters*, *153*(1-2), 103–118. https://doi.org/10.1016/S0012-821X(97)00164-7

Chen, T., Robinson, L. F., Burke, A., Southon, J., Spooner, P., Morris, P. J., & Ng, H. C. (2015). Synchronous centennial abrupt events in the ocean and atmosphere during the last deglaciation. *Science*, *349*(6255), 1537–1541. https://doi.org/10.1126/science.aac6159

Cheng, H., Edwards, R. L., Broecker, W. S., Denton, G. H., Kong, X. G., Wang, Y. J., et al. (2009). Ice age terminations. *Science*, *326*(5950), 248–252. https://doi.org/10.1126/science.1177840

Cheng, H., Edwards, R. L., Sinha, A., Spötl, C., Yi, L., Chen, S., et al. (2016). The Asian monsoon over the past 640,000 years and ice age terminations. *Nature*, *534*(7609), 640–646. https://doi.org/10.1038/nature18591

Deaney, E. D., Barker, S., & Van de Flierdt, T. (2017). Timing and nature of AMOC recovery across Termination 2 and magnitude of deglacial CO_2 change. *Nature Communications*, *8*(1). https://doi.org/10.1038/NCOMMS14595

Denton, G. H., Anderson, R. F., Toggweiler, J. R., Edwards, R. L., Schaefer, J. M., & Putnam, A. E. (2010). The last glacial termination. *Science*, *328*(5986), 1652–1656. https://doi.org/10.1126/science.1184119

Dickson, R. R., & Brown, J. (1994). The production of North-Atlantic deep-water—Sources, rates, and pathways. *Journal of Geophysical Research*, *99*(C6), 12,319–12,341. https://doi.org/10.1029/94JC00530

Dima, M., & Lohmann, G. (2010). Evidence for two distinct modes of large-scale ocean circulation changes over the last century. *Journal of Climate*, *23*(1), 5–16. https://doi.org/10.1175/2009JCLI2867.1

Elderfield, H., Ferretti, P., Greaves, M., Crowhurst, S., McCave, I. N., Hodell, D., & Piotrowski, A. M. (2012). Evolution of ocean temperature and ice volume through the mid-pleistocene climate transition. *Science*, *337*(6095), 704–709. https://doi.org/10.1126/science.1221294

Elsig, J., Schmitt, J., Leuenberger, D., Schneider, R., Eyer, M., Leuenberger, M., et al. (2009). Stable isotope constraints on Holocene carbon cycle changes from an Antarctic ice core. *Nature*, *461*(7263), 507–510. https://doi.org/10.1038/nature08393

Evans, H. B. (1965). GRAPE*-A device for continuous determination of material density and porosity, paper presented at SPWLA 6th annual logging symposium (Volume II), Society of Petrophysicists and Well-Log Analysts.

Eynaud, F. (2011). Planktonic foraminifera in the Arctic: Potentials and issues regarding modern and quaternary populations. *IOP Conference Series: Earth and Environmental Science*, *14*(1), 12,005. https://doi.org/10.1088/1755-1315/14/1/012005

Ezat, M. M., Rasmussen, T. L., & Groeneveld, J. (2014). Persistent intermediate water warming during cold stadials in the southeastern Nordic seas during the past 65 k.y. *Geology*, *42*(8), 663–666. https://doi.org/10.1130/G35579.1

Ganopolski, A., & Brovkin, V. (2017). Simulation of climate, ice sheets and CO2 evolution during the last four glacial cycles with an Earth system model of intermediate complexity. *Climate of the Past*, *13*(12), 1695–1716. https://doi.org/10.5194/cp-13-1695-2017

Grinsted, A., Moore, J. C., & Jevrejeva, S. (2004). Application of the cross wavelet transform and wavelet coherence to geophysical time series. *Nonlinear Processes in Geophysics*, *11*(5/6), 561–566.

Heinrich, H. (1988). Origin and consequences of cyclic ice rafting in the Northeast Atlantic Ocean during the past 130,000 years. *Quaternary Research*, *29*(2), 142–152. https://doi.org/10.1016/0033-5894(88)90057-9

Hemming, S. R. (2004). Heinrich events: Massive late pleistocene detritus layers of the North Atlantic and their global climate imprint. *Reviews of Geophysics*, *42*, RG1005. https://doi.org/10.1029/2003RG000128

Henry, L., McManus, J. F., Curry, W. B., Roberts, N. L., Piotrowski, A. M., & Keigwin, L. D. (2016). North Atlantic ocean circulation and abrupt climate change during the last glaciation. *Science*, *353*(6298), 470–474. https://doi.org/10.1126/science.aaf5529

Hodell, D., Lourens, L., Crowhurst, S., Konijnendijk, T., Tjallingii, R., Jiménez-Espejo, F., et al. (2015). A reference time scale for Site U1385 (Shackleton Site) on the SW Iberian Margin. *Global and Planetary Change*, *133*, 49–64. https://doi.org/10.1016/j.gloplacha.2015.07.002

Hodell, D. A., Channell, J. E. T., Curtis, J. H., Romero, O. E., & Roehl, U. (2008). Onset of "Hudson Strait" Heinrich events in the eastern North Atlantic at the end of the middle Pleistocene transition (similar to 640 ka)? *Paleoceanography*, *23*, PA4218. https://doi.org/10.1029/2008PA001591

Hodell, D. A., Minth, E. K., Curtis, J. H., McCave, I. N., Hall, I. R., Channell, J. E. T., & Xuan, C. (2009). Surface and deep-water hydrography on Gardar Drift (Iceland Basin) during the last interglacial period. *Earth and Planetary Science Letters*, *288*(1-2), 10–19. https://doi.org/10.1016/j.epsl.2009.08.040

Hoffman, J. S., Clark, P. U., Parnell, A. C., & He, F. (2017). Regional and global sea-surface temperatures during the last interglaciation. *Science*, *355*(6322), 276–279. https://doi.org/10.1126/science.aai8464

Imbrie, J., Berger, A., Boyle, E. A., Clemens, S. C., Duffy, A., Howard, W. R., et al. (1993). On the structure and origin of major glaciation cycles 2. the 100,000-year cycle. *Paleoceanography*, *8*(6), 699–735. https://doi.org/10.1029/93PA02751

Imbrie, J., Boyle, E. A., Clemens, S. C., Duffy, A., Howard, W. R., Kukla, G., et al. (1992). On the structure and origin of major glaciation cycles 1. Linear responses to Milankovitch forcing. *Paleoceanography*, *7*(6), 701–738. https://doi.org/10.1029/92PA02253

Indermühle, A., Stocker, T. F., Joos, F., Fischer, H., Smith, H. J., Wahlen, M., et al. (1999). Holocene carbon-cycle dynamics based on CO_2 trapped in ice at Taylor Dome, Antarctica. *Nature*, *398*(6723), 121–126. https://doi.org/10.1038/18158

Jansen, E., Raymo, M. E., & Blum, P. (1996). Proceedings of the Ocean Drilling Program, Initial Reports (Vol. 162). Texas A & M University, Ocean Drilling Program.

Jansen, M. F., Nadeau, L. P., & Merlis, T. M. (2018). Transient versus equilibrium response of the ocean's overturning circulation to warming. *Journal of Climate*, *31*(13), 5147–5163. https://doi.org/10.1175/jcli-d-17-0797.1

Jouzel, J., Masson-Delmotte, V., Cattani, O., Dreyfus, G., Falourd, S., Hoffmann, G., et al. (2007). Orbital and millennial Antarctic climate variability over the past 800,000 years. *Science*, *317*(5839), 793–796. https://doi.org/10.1126/science.1141038

Kleinen, T., Brovkin, V., von Bloh, W., Archer, D., & Munhoven, G. (2010). Holocene carbon cycle dynamics. *Geophysical Research Letters*, *37*, L02705. https://doi.org/10.1029/2009GL041391

Kleiven, H. F., Hall, I. R., McCave, I. N., Knorr, G., & Jansen, E. (2011). Coupled deep-water flow and climate variability in the middle Pleistocene North Atlantic. *Geology*, *39*(4), 343–346. https://doi.org/10.1130/G31651.1

Knorr, G., & Lohmann, G. (2007). Rapid transitions in the Atlantic thermohaline circulation triggered by global warming and meltwater during the last deglaciation. *Geochemistry, Geophysics, Geosystems*, *8*, Q12006. https://doi.org/10.1029/2007GC001604

Kohler, P., Fischer, H., Munhoven, G., & Zeebe, R. E. (2005). Quantitative interpretation of atmospheric carbon records over the last glacial termination. *Global Biogeochemical Cycles*, *19*, GB4020. https://doi.org/10.1029/2004GB002345

Lehman, S. J., & Keigwin, L. D. (1992). Sudden changes in North Atlantic circulation during the last deglaciation. *Nature*, *356*(6372), 757–762. https://doi.org/10.1038/356757a0

Lisiecki, L. E., & Raymo, M. E. (2005). A Pliocene-Pleistocene stack of 57 globally distributed benthic $\delta^{18}O$ records. *Paleoceanography*, *20*, PA1003. https://doi.org/10.1029/2004PA001071

Liu, Z., Otto-Bliesner, B. L., He, F., Brady, E. C., Tomas, R., Clark, P. U., et al. (2009). Transient simulation of last deglaciation with a new mechanism for Bolling-Allerod warming. *Science*, *325*(5938), 310–314. https://doi.org/10.1126/science.1171041

Locarnini, R. A., Mishonov, A. V., Antonov, J. I., Boyer, T. P., Garcia, H. E., Baranova, O. K., Zweng, M. M., & Johnson, D. R. (2010). World Ocean Atlas 2009, Volume 1: Temperature. In S. Levitus (Ed.), *NOAA Atlas NESDIS* (Vol. 68, p. 184). Washington, DC: U.S. Government Printing Office.

Loulergue, L., Schilt, A., Spahni, R., Masson-Delmotte, V., Blunier, T., Lemieux, B., et al. (2008). Orbital and millennial-scale features of atmospheric CH_4 over the past 800,000 years. *Nature*, *453*(7193), 383–386. https://doi.org/10.1038/nature06950

Marchal, O., Stocker, T. F., & Joos, F. (1998). Impact of oceanic reorganizations on the ocean carbon cycle and atmospheric carbon dioxide content. *Paleoceanography*, *13*(3), 225–244. https://doi.org/10.1029/98PA00726

Marcott, S. A., Bauska, T. K., Buizert, C., Steig, E. J., Rosen, J. L., Cuffey, K. M., et al. (2014). Centennial-scale changes in the global carbon cycle during the last deglaciation. *Nature*, *514*(7524), 616–619. https://doi.org/10.1038/nature13799

Margo_Project_Members (2009). Constraints on the magnitude and patterns of ocean cooling at the Last Glacial Maximum. *Nature Geoscience*, *2*(2), 127–132. https://doi.org/10.1038/ngeo411

Martrat, B., Grimalt, J. O., Shackleton, N. J., de Abreu, L., Hutterli, M. A., & Stocker, T. F. (2007). Four climate cycles of recurring deep and surface water destabilizations on the Iberian margin. *Science*, *317*(5837), 502–507. https://doi.org/10.1126/science.1139994

Masson-Delmotte, V., Stenni, B., Pol, K., Braconnot, P., Cattani, O., Falourd, S., et al. (2010). EPICA Dome C record of glacial and interglacial intensities. *Quaternary Science Reviews*, *29*(1-2), 113–128. https://doi.org/10.1016/j.quascirev.2009.09.030

McManus, J. F., Francois, R., Gherardi, J. M., Keigwin, L. D., & Brown-Leger, S. (2004). Collapse and rapid resumption of Atlantic meridional circulation linked to deglacial climate changes. *Nature*, *428*(6985), 834–837. https://doi.org/10.1038/nature02494

McManus, J. F., Oppo, D. W., & Cullen, J. L. (1999). A 0.5-million-year record of millennial-scale climate variability in the North Atlantic. *Science*, *283*(5404), 971–975.

Menviel, L., England, M. H., Meissner, K., Mouchet, A., & Yu, J. (2014). Atlantic-Pacific seesaw and its role in outgassing CO_2 during Heinrich events. *Paleoceanography*, *29*, 58–70. https://doi.org/10.1002/2013PA002542

Menviel, L., Timmermann, A., Mouchet, A., & Timm, O. (2008). Meridional reorganizations of marine and terrestrial productivity during Heinrich events. *Paleoceanography*, *23*, PA1203. https://doi.org/10.1029/2007PA001445

Milankovitch, M. (1941). *Kanon der Erdbestrahlung und seine Andwendung auf das Eiszeiten-problem*. Belgrade: Royal Serbian Academy.

Muir, L., & Fedorov, A. (2015). How the AMOC affects ocean temperatures on decadal to centennial timescales: The North Atlantic versus an interhemispheric seesaw. *Climate Dynamics*, *45*(1-2), 151–160. https://doi.org/10.1007/s00382-014-2443-7

Naafs, B. D. A., Hefter, J., Ferretti, P., Stein, R., & Haug, G. H. (2011). Sea surface temperatures did not control the first occurrence of Hudson Strait Heinrich Events during MIS 16. *Paleoceanography*, *26*, PA4201. https://doi.org/10.1029/2011PA002135

NGRIP_members (2004). High-resolution record of Northern Hemisphere climate extending into the last interglacial period. *Nature*, *431*(7005), 147–151. https://doi.org/10.1038/nature02805

Oppo, D. W., McManus, J. F., & Cullen, J. L. (1998). Abrupt climate events 500,000 to 340,000 years ago: Evidence from subpolar north Atlantic sediments. *Science*, *279*(5355), 1335–1338. https://doi.org/10.1126/science.279.5355.1335

Parrenin, F., Barker, S., Blunier, T., Chappellaz, J., Jouzel, J., Landais, A., et al. (2012). On the gas-ice depth difference (Δdepth) along the EPICA Dome C ice core. *Climate of the Past*, *8*(4), 1239–1255. https://doi.org/10.5194/cp-8-1239-2012

PIGS_working_group (2016), Interglacials of the last 800,000 years.

Piotrowski, A. M., Goldstein, S. L., Hemming, S. R., & Fairbanks, R. G. (2005). Temporal relationships of carbon cycling and ocean circulation at glacial boundaries. *Science*, *307*(5717), 1933–1938. https://doi.org/10.1126/science.1104883

Rahmstorf, S., Box, J. E., Feulner, G., Mann, M. E., Robinson, A., Rutherford, S., & Schaffernicht, E. J. (2015). Exceptional twentieth-century slowdown in Atlantic Ocean overturning circulation. *Nature Climate Change*, *5*(5), 475–480. https://doi.org/10.1038/nclimate2554

Raymo, M. E., Oppo, D. W., Flower, B. P., Hodell, D. A., McManus, J. F., Venz, K. A., et al. (2004). Stability of North Atlantic water masses in face of pronounced climate variability during the Pleistocene. *Paleoceanography*, *19*, PA2008. https://doi.org/10.1029/2003PA000921

Ridgwell, A. J., Watson, A. J., Maslin, M. A., & Kaplan, J. O. (2003). Implications of coral reef buildup for the controls on atmospheric CO_2 since the Last Glacial Maximum. *Paleoceanography*, *18*(4), 1083. https://doi.org/10.1029/2003PA000893

Roberts, N. L., Piotrowski, A. M., McManus, J. F., & Keigwin, L. D. (2010). Synchronous deglacial overturning and water mass source changes. *Science*, *327*(5961), 75–78. https://doi.org/10.1126/science.1178068

Rohling, E. J., Braun, K., Grant, K., Kucera, M., Roberts, A., Siddall, M., & Trommer, G. (2010). Comparison between Holocene and Marine Isotope Stage-11 sea-level histories. *Earth and Planetary Science Letters*, *291*(1-4), 97–105. https://doi.org/10.1016/j.epsl.2009.12.054

Ruddiman, W., Fuller, D., Kutzbach, J., Tzedakis, P., Kaplan, J., Ellis, E., et al. (2016). Late Holocene climate: Natural or anthropogenic? *Reviews of Geophysics*, *54*, 93–118. https://doi.org/10.1002/2015RG000503

Ruddiman, W. F. (2003). The anthropogenic greenhouse era began thousands of years ago. *Climatic Change*, *61*(3), 261–293.

Schlitzer, R. (2014). Ocean Data View. http://odv.awi.de

Schmittner, A., & Galbraith, E. D. (2008). Glacial greenhouse-gas fluctuations controlled by ocean circulation changes. *Nature*, *456*(7220), 373–376. https://doi.org/10.1038/nature07531

Schmittner, A., Saenko, O. A., & Weaver, A. J. (2003). Coupling of the hemispheres in observations and simulations of glacial climate change. *Quaternary Science Reviews*, *22*(5-7), 659–671. https://doi.org/10.1016/S0277-3791(02)00184-1

Shackleton, N. J. (2000). The 100,000-year ice-age cycle identified and found to lag temperature, carbon dioxide, and orbital eccentricity. *Science*, *289*(5486), 1897–1902. https://doi.org/10.1126/science.289.5486.1897

Shackleton, N. J., Hall, M. A., & Vincent, E. (2000). Phase relationships between millennial-scale events 64,000-24,000 years ago. *Paleoceanography*, *15*(6), 565–569. https://doi.org/10.1029/2000PA000513

Shaffer, G., Olsen, S. M., & Bjerrum, C. J. (2004). Ocean subsurface warming as a mechanism for coupling Dansgaard-Oeschger climate cycles and ice-rafting events. *Geophysical Research Letters*, *31*, L24202. https://doi.org/10.1029/2004GL020968

Shakun, J. D., Clark, P. U., He, F., Marcott, S. A., Mix, A. C., Liu, Z., et al. (2012). Global warming preceded by increasing carbon dioxide concentrations during the last deglaciation. *Nature*, *484*(7392), 49–54. https://doi.org/10.1038/nature10915

Sigman, D. M., Hain, M. P., & Haug, G. H. (2010). The polar ocean and glacial cycles in atmospheric CO_2 concentration. *Nature*, *466*(7302), 47–55. https://doi.org/10.1038/nature09149

Sima, A., Paul, A., & Schulz, M. (2004). The Younger Dryas—An intrinsic feature of late Pleistocene climate change at millennial timescales. *Earth Planet. Sci. Lett.*, *222*(3-4), 741–750. https://doi.org/10.1016/j.epsl.2004.03.026

Skinner, L., & Elderfield, H. (2007). Rapid fluctuations in the deep North Atlantic heat budget during the last glacial period. *Paleoceanography*, *22*, PA1205. https://doi.org/10.1029/2006PA001338

Skinner, L. C., Fallon, S., Waelbroeck, C., Michel, E., & Barker, S. (2010). Ventilation of the deep Southern Ocean and deglacial CO_2 rise. *Science*, *328*(5982), 1147–1151. https://doi.org/10.1126/science.1183627

Smeed, D., Josey, S., Beaulieu, C., Johns, W., Moat, B., Frajka-Williams, E., et al. (2018). The North Atlantic Ocean is in a state of reduced overturning. *Geophysical Research Letters*, *45*, 1527–1533. https://doi.org/10.1002/2017GL076350

Smith, D., Harrison, S., Firth, C. R., & Jordan, J. T. (2011). The early Holocene sea level rise. *Quaternary Science Reviews*, *30*(15-16), 1846–1860. https://doi.org/10.1016/j.quascirev.2011.04.019

Stocker, T. F., & Johnsen, S. J. (2003). A minimum thermodynamic model for the bipolar seesaw. *Paleoceanography*, *18*(4), 1087. https://doi.org/10.1029/2003PA000920

Thornalley, D. J., Blaschek, M., Davies, F. J., Praetorius, S., Oppo, D. W., McManus, J. F., et al. (2013). Long-term variations in Iceland–Scotland overflow strength during the Holocene. *Climate of the Past Discussions*, *9*(2), 1627–1656. https://doi.org/10.5194/cpd-9-1627-2013

Thornalley, D. J., Oppo, D. W., Ortega, P., Robson, J. I., Brierley, C. M., Davis, R., et al. (2018). Anomalously weak Labrador Sea convection and Atlantic overturning during the past 150 years. *Nature*, *556*(7700), 227–230. https://doi.org/10.1038/s41586-018-0007-4

Thornalley, D. J. R., Elderfield, H., & McCave, I. N. (2010). Intermediate and deep water paleoceanography of the northern North Atlantic over the past 21,000 years. *Paleoceanography*, *25*, PA1211. https://doi.org/10.1029/2009PA001833

Tzedakis, P., Crucifix, M., Mitsui, T., & Wolff, E. W. (2017). A simple rule to determine which insolation cycles lead to interglacials. *Nature*, *542*(7642), 427–432. https://doi.org/10.1038/nature21364

Tzedakis, P., Raynaud, D., McManus, J., Berger, A., Brovkin, V., & Kiefer, T. (2009). Interglacial diversity. *Nature Geoscience*, *2*(11), 751–755 . https://doi.org/10.1038/ngeo660

Tzedakis, P., Wolff, E., Skinner, L., Brovkin, V., Hodell, D., McManus, J. F., & Raynaud, D. (2012). Can we predict the duration of an interglacial? *Climate of the Past*, *8*(5), 1473–1485. https://doi.org/10.5194/cp-8-1473-2012

Venz, K. A., Hodell, D. A., Stanton, C., & Warnke, D. A. (1999). A 1.0 Myr record of glacial North Atlantic intermediate water variability from ODP site 982 in the northeast Atlantic. *Paleoceanography*, *14*(1), 42–52.

Veres, D., Bazin, L., Landais, A., Kele, H. T. M., Lemieux-Dudon, B., Parrenin, F., et al. (2012). The Antarctic ice core chronology (AICC2012): An optimized multi-parameter and multi-site dating approach for the last 120 thousand years. *Climate of the Past Discussions*, *8*(6), 6011–6049. https://doi.org/10.5194/cpd-8-6011-2012

Weber, S. L., Drijfhout, S. S., Abe-Ouchi, A., Crucifix, M., Eby, M., Ganopolski, A., et al. (2007). The modern and glacial overturning circulation in the Atlantic Ocean in PMIP coupled model simulations. *Climate of the Past*, *3*(1), 51–64. https://doi.org/10.5194/cp-3-51-2007

Wunsch, C. (2006). Abrupt climate change: An alternative view. *Quaternary Research*, *65*(02), 191–203. https://doi.org/10.1016/j.yqres.2005.10.006

Yang, H. J., & Zhu, J. (2011). Equilibrium thermal response timescale of global oceans. *Geophysical Research Letters*, *38*, L14711. https://doi.org/10.1029/2011GL048076

Zahn, R. (1994). Core correlations. *Nature*, *371*(6495), 289–290. https://doi.org/10.1038/371289a0

Zhang, R. (2008). Coherent surface-subsurface fingerprint of the Atlantic meridional overturning circulation. *Geophysical Research Letters*, *35*, L20705. https://doi.org/10.1029/2008GL035463

Zhang, X., Knorr, G., Lohmann, G., & Barker, S. (2017). Abrupt North Atlantic circulation changes in response to gradual CO_2 forcing in a glacial climate state. *Nature Geoscience*, *10*(7), 518–523. https://doi.org/10.1038/ngeo2974

Zhang, X., Lohmann, G., Knorr, G., & Purcell, C. (2014). Abrupt glacial climate shifts controlled by ice sheet changes. *Nature*, *512*(7514), 290–294. https://doi.org/10.1038/nature13592